MINISTÉRIO DO EQUIPAMENTO SOCIAL

Laboratório Nacional de Engenharia Civil

NÃO CONFIDENCIAL

DEPARTAMENTO DE VIAS DE COMUNICAÇÃO

Núcleo de Pavimentos Rodoviários

Proc. 092/19/13267

DEPARTAMENTO DE BARRAGENS

Núcleo de Dimensionamento Experimental e de Estudos Especiais

Proc. Int. 042/533/456

COST 334 - EFFECTS OF WIDE TYRES AND DUAL TYRES

Task Group 3 - Pavement wear effects

Mechanistic approach for rutting - Stage 4

RELATÓRIO 244/2000 - NPR/NDE/NEE

Lisboa, June 2000

I&D
VIAS DE COMUNICAÇÃO/BARRAGENS

COST 334 – EFFECTS OF WIDE TYRES AND DUAL TYRES
Task Group 3 – Pavement wear effects

Mechanistic approach for rutting – Stage 4

COST 334 – ESTUDO COMPARATIVO DO EFEITO DE RODADOS SIMPLES DE BASE LARGA E DE RODADOS DUPLOS
Grupo de Trabalho 3 – Efeito no consumo do pavimento

Previsão de cavados de rodeira – Fase 4

COST 334 – EFFETS DE ROUES SIMPLES LARGES ET DE JUMELAGES
Groupe de Travail 3 – Effets dans la consommation des chaussées

Prévision d'ornières – Phase 4

COST 334 – EFFECTS OF WIDE TYRES AND DUAL TYRES
Task Group 3 – Pavement wear effects

Mechanistic approach for rutting – Stage 4

TABLE OF CONTENTS

INDEX OF FIGURES

INDEX OF TABLES

COST 334 – EFFECTS OF WIDE TYRES AND DUAL TYRES
Task Group 3 – Pavement wear effects

Mechanistic approach for rutting – Stage 4

1 - INTRODUCTION

Action COST 334 (*Effects of wide single tyres and dual tyres*) aims at a better understanding of the overall effects of the widespread, and increasing use, of wide single tyres for heavy goods vehicles in Europe.

Within Task 3 (*Pavement wear effects*) a research program has been set up to evaluate the relative wear effects on pavements of wide base single and dual tyres.

The National Laboratory for Civil Engineering (LNEC) was engaged in a contribution for this research program for the evaluation of rutting using a mechanistic approach. The computational code used to perform the viscoelastic calculations was CREEPN, developed at LNEC.

CREEPN is a 3D finite element code that allows to model the material in a linear viscoelastic behaviour expressed by the Burgers' model. The program uses elements of volume with sixteen nodes (Batista,1998).

The contribution of LNEC has been programmed in four stages:

Stage 1 – Predicting, by CREEPN, of rutting measured in laboratory wheel tracking tests of a bituminous mixture. The viscoelastic characteristics of this bituminous mixture were evaluated in repeated uniaxial loading tests;

– Comparing the results from CREEPN with the results from VEROAD. Some additional calculations were performed with the widespread code DIANA that uses an approach similar to CREEPN;

Stage 2 – Validating the CREEPN approach with existent results of tests performed at TRL (UK) and LCPC (F);

Stage 3 – Validating the CREEPN approach with tests to be performed at TRL (UK) and LINTRACK (NL) in the context of Task Group 3;

Stage 4 – Performing additional calculations to allow a comparison of the relative potential for permanent deformation concerning:

- Dual Tyres versus Wide Single Tyre
- Magnitude of the inflation pressure
- Size of the contact area
- Unequal load sharing

The research carried out under Stage 1 and Stage 2 was reported previously (Quaresma et al., 2000).

This report presents the research for the Stage 4.

2 - DATA FOR CREEPN CALCULATIONS

Table 1 shows the load characteristics (tyre contact area and contact pressure) that were used in CREEPN. For the calculations to evaluate the effect of unbalanced loads in a dual tyre assembly, a 25% higher contact pressure for one wheel and a 25% lower contact pressure for the other wheel was used.

Table 1 – Load characteristics (Penant, 1999)

Tyre code	Axle load (ton)	Inflation pressure (bar)	Width (mm)	Length (mm)	Contact pressure (kNm^{-2})	Ratio Contact/Inflation (%)
295/60R22.5	9.0	8	259	170	501.1	63.9
295/60R22.5	11.5	10	259	174	625.6	63.8
295/80R22.5	9.0	7	244	194	466.1	67.9
315/80R22.5	9.0	6.5	255	185	467.7	73.4
315/80R22.5	11.5	8	255	193	572.9	73.0
385/65R22.5	9.0	10	283	201	775.8	79.1
495/45R22.5	9.0	8	428	176	585.8	74.7
495/45R22.5	11.5	10	428	180	731.9	74.6

Figure 1 shows the finite element mesh for CREEPN (only asphalt layers). All nodes in the base are fixed and the lateral nodes are fixed only in the perpendicular direction.

This computer simulation was done for one cycle (1 pass). The speed used in test was 13.89 ms^{-1} (50 km/h).

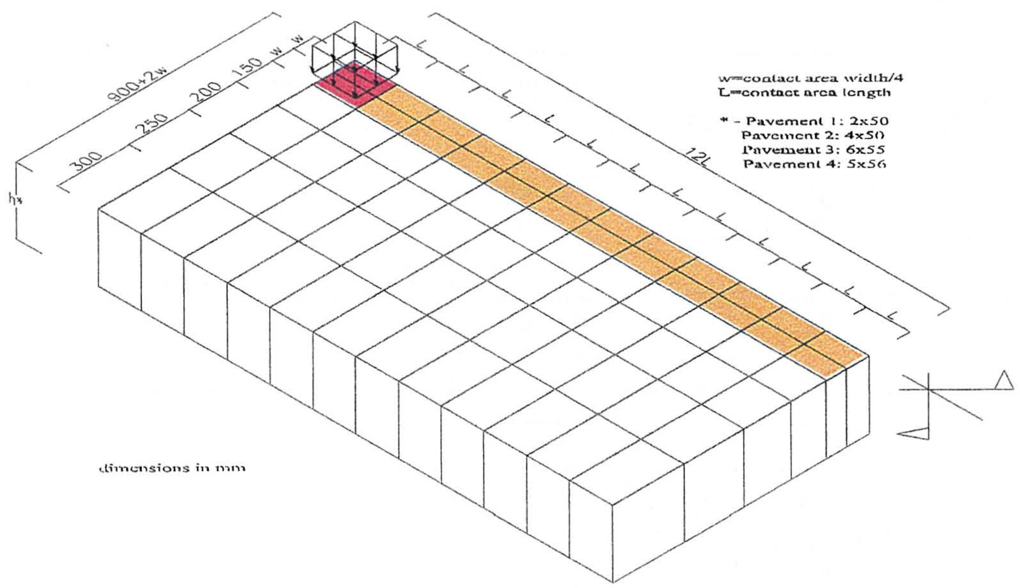

Figure 1 – Finite element mesh used in CREEPN

Table 2 shows the material properties for the layers of the different structures used in CREEPN calculations.

Table 2 – Material properties for the layers of the different structures

Layers characteristics		Structure 1	Structure 2	Structure 3	Structure 4
Asphalt layer	thickness (mm)	100	200	330	280
	Burgers' serial damper parameter ($MNm^{-2}s$)	3000			
	Poisson's ratio	0.40			
Granular layer	thickness (mm)	300	250	200	
	Young's modulus (MNm^{-2})	200			
	Poisson's ratio	0.35			
Cement bound base	thickness (mm)				200
	Young's modulus (MNm^{-2})				10000
	Poisson's ratio				0.20
Foundation	Young's modulus (MNm^{-2})	70			
	Poisson's ratio	0.35			

Figure 2 shows the different structures presented in Table 2.

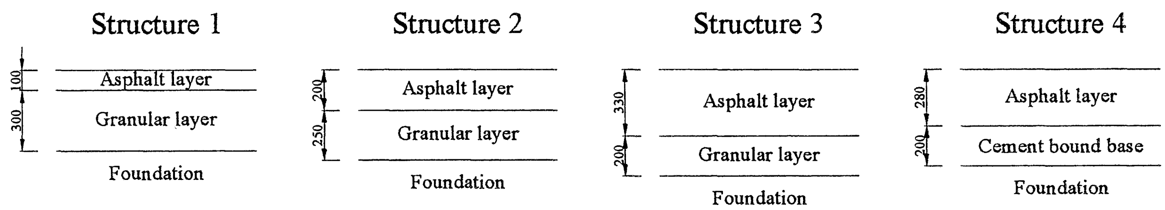

Figure 2 – Structures used in CREEPN

Figure 3 shows the lateral distribution model that was used to take into account the lateral wandering. To obtain this lateral distribution was used a modified Laplace distribution (Metcalfe, 1997).

$$f(x) = \frac{1}{2\lambda} e^{-\left|\frac{x}{\lambda}\right|} \times C$$

Where λ=0.08 and C=4000.

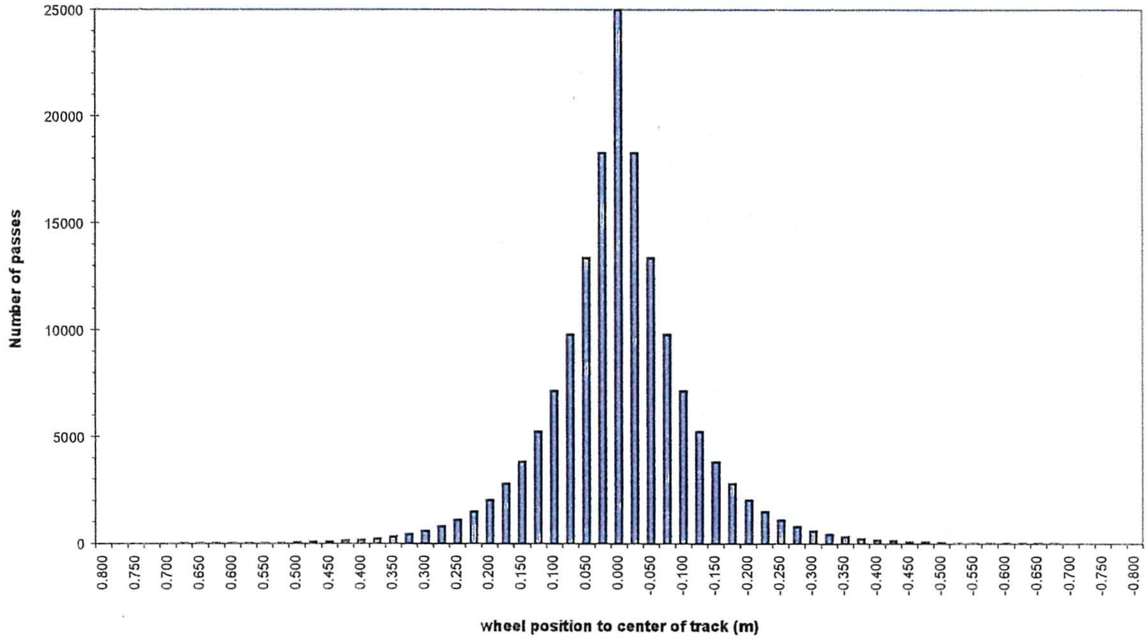

Figure 3 – Laplace distribution for lateral wandering

3 - RESULTS FROM CREEPN

Figure 4 shows the permanent deformation parameters that were calculated with CREEPN code and Table 3, Table 4, Table 5 and Table 6 show the results for these parameters.

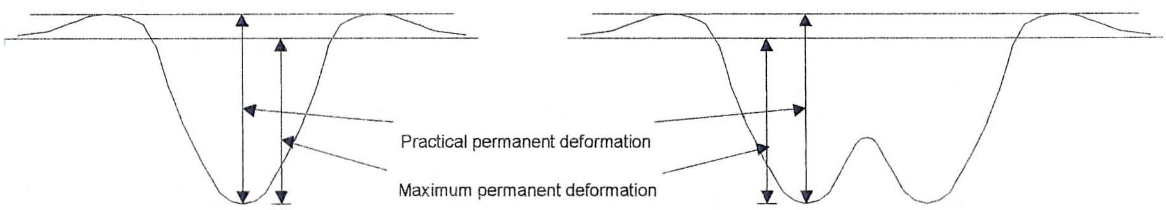

Figure 4 – Parameters that were analysed in CREEPN

Table 3 – Maximum permanent deformation without the effect of lateral wandering

Maximum permanent deformation at surface without lateral wander (mm/cycle)					
Tyre size		Structure 1	Structure 2	Structure 3	Structure 4
295/60R22.5 (9.0 ton / 8 bar)	Balanced	0.000113	0.000225	0.000350	0.000303
	Unbalanced	0.000139	0.000287	0.000440	0.000385
295/60R22.5 (11.5 ton / 10 bar)	Balanced	0.000143	0.000288	0.000447	0.000387
	Unbalanced	0.000178	0.000368	0.000562	0.000493
295/80R22.5 (9.0 ton / 7 bar)	Balanced	0.000119	0.000237	0.000363	0.000315
	Unbalanced	0.000149	0.000304	0.000457	0.000402
315/80R22.5 (9.0 ton / 6.5 bar)	Balanced	0.000114	0.000228	0.000354	0.000306
	Unbalanced	0.000142	0.000292	0.000445	0.000390
315/80R22.5 (11.5 ton / 8 bar)	Balanced	0.000146	0.000291	0.000451	0.000391
	Unbalanced	0.000181	0.000373	0.000567	0.000498
385/65R22.5 (9.0 ton / 10 bar)		0.000201	0.000438	0.000676	0.000594
495/45R22.5 (9.0 ton / 8 bar)		0.000130	0.000283	0.000478	0.000406
495/45R22.5 (11.5 ton / 10 bar)		0.000167	0.000362	0.000611	0.000519

Table 4 – Maximum permanent deformation with the effect of lateral wandering

Maximum permanent deformation at surface with lateral wander (mm/cycle)					
Tyre size		Structure 1	Structure 2	Structure 3	Structure 4
295/60R22.5 (9.0 ton / 8 bar)	Balanced	0.000089	0.000181	0.000295	0.000252
	Unbalanced	0.000110	0.000226	0.000361	0.000311
295/60R22.5 (11.5 ton / 10 bar)	Balanced	0.000114	0.000232	0.000377	0.000322
	Unbalanced	0.000140	0.000289	0.000462	0.000397
295/80R22.5 (9.0 ton / 7 bar)	Balanced	0.000092	0.000186	0.000300	0.000257
	Unbalanced	0.000114	0.000233	0.000368	0.000318
315/80R22.5 (9.0 ton / 6.5 bar)	Balanced	0.000090	0.000182	0.000297	0.000253
	Unbalanced	0.000111	0.000228	0.000363	0.000312
315/80R22.5 (11.5 ton / 8 bar)	Balanced	0.000115	0.000233	0.000379	0.000323
	Unbalanced	0.000142	0.000292	0.000464	0.000399
385/65R22.5 (9.0 ton / 10 bar)		0.000162	0.000345	0.000544	0.000473
495/45R22.5 (9.0 ton / 8 bar)		0.000114	0.000253	0.000426	0.000363
495/45R22.5 (11.5 ton / 10 bar)		0.000146	0.000324	0.000544	0.000464

Table 5 – Practical permanent deformation without the effect of lateral wandering

Practical permanent deformation at surface without lateral wander (mm/cycle)					
Tyre size		Structure 1	Structure 2	Structure 3	Structure 4
295/60R22.5 (9.0 ton / 8 bar)	Balanced	0.000127	0.000240	0.000380	0.000329
	Unbalanced	0.000154	0.000304	0.000471	0.000413
295/60R22.5 (11.5 ton / 10 bar)	Balanced	0.000160	0.000308	0.000486	0.000421
	Unbalanced	0.000197	0.000389	0.000602	0.000529
295/80R22.5 (9.0 ton / 7 bar)	Balanced	0.000137	0.000253	0.000395	0.000343
	Unbalanced	0.000169	0.000321	0.000490	0.000432
315/80R22.5 (9.0 ton / 6.5 bar)	Balanced	0.000130	0.000243	0.000384	0.000333
	Unbalanced	0.000160	0.000309	0.000476	0.000418
315/80R22.5 (11.5 ton / 8 bar)	Balanced	0.000167	0.000311	0.000490	0.000425
	Unbalanced	0.000204	0.000394	0.000608	0.000534
385/65R22.5 (9.0 ton / 10 bar)		0.000230	0.000467	0.000721	0.000637
495/45R22.5 (9.0 ton / 8 bar)		0.000149	0.000305	0.000517	0.000440
495/45R22.5 (11.5 ton / 10 bar)		0.000191	0.000389	0.000660	0.000563

Table 6 – Practical permanent deformation with the effect of lateral wandering

Practical permanent deformation at surface with lateral wander (mm/cycle)					
Tyre size		Structure 1	Structure 2	Structure 3	Structure 4
295/60R22.5 (9.0 ton / 8 bar)	Balanced	0.000088	0.000187	0.000317	0.000268
	Unbalanced	0.000109	0.000232	0.000383	0.000327
295/60R22.5 (11.5 ton / 10 bar)	Balanced	0.000114	0.000240	0.000404	0.000342
	Unbalanced	0.000140	0.000298	0.000489	0.000417
295/80R22.5 (9.0 ton / 7 bar)	Balanced	0.000092	0.000193	0.000322	0.000272
	Unbalanced	0.000114	0.000240	0.000390	0.000334
315/80R22.5 (9.0 ton / 6.5 bar)	Balanced	0.000089	0.000188	0.000319	0.000269
	Unbalanced	0.000110	0.000234	0.000385	0.000328
315/80R22.5 (11.5 ton / 8 bar)	Balanced	0.000115	0.000241	0.000407	0.000343
	Unbalanced	0.000142	0.000300	0.000492	0.000419
385/65R22.5 (9.0 ton / 10 bar)		0.000162	0.000355	0.000572	0.000494
495/45R22.5 (9.0 ton / 8 bar)		0.000114	0.000262	0.000451	0.000381
495/45R22.5 (11.5 ton / 10 bar)		0.000146	0.000336	0.000575	0.000488

4 - DISCUSSION OF THE RESULTS

The comparison of the results obtained by CREEPN for the different tyres is made in terms of a relative pavement wear in terms of rutting due to permanent deformation of asphalt layers.

As a reference for relative pavement primary rutting it was considered a 11.5 ton axle 315/80R22.5 dual tyre with an 8 bar inflation pressure. Table 7 presents the relative pavement primary rutting, in terms of the practical permanent deformation with the effect of lateral wandering.

Table 7 – Relative pavement primary rutting (Reference 11.5 ton 315/80R22.5 dual tyre)

Relative pavement primary rutting for the practical permanent deformation at surface with lateral wander					
Tyre size		**Structure 1**	**Structure 2**	**Structure 3**	**Structure 4**
295/60R22.5 (9.0 ton / 8 bar)	Balanced	0.37	0.78	1.32	1.11
	Unbalanced	0.45	0.96	1.59	1.36
295/60R22.5 (11.5 ton / 10 bar)	Balanced	0.47	1.00	1.68	1.42
	Unbalanced	0.58	1.24	2.03	1.73
295/80R22.5 (9.0 ton / 7 bar)	Balanced	0.38	0.80	1.34	1.13
	Unbalanced	0.47	1.00	1.62	1.39
315/80R22.5 (9.0 ton / 6.5 bar)	Balanced	0.37	0.78	1.32	1.12
	Unbalanced	0.46	0.97	1.60	1.36
315/80R22.5 (11.5 ton / 8 bar)	Balanced	0.48	**1.00**	1.69	1.42
	Unbalanced	0.59	1.24	2.04	1.74
385/65R22.5 (9.0 ton / 10 bar)		0.67	1.47	2.37	2.05
495/45R22.5 (9.0 ton / 8 bar)		0.47	1.09	1.87	1.58
495/45R22.5 (11.5 ton / 10 bar)		0.61	1.39	2.39	2.02

4.1 - Unequal load sharing

For the unbalanced loads in tyres 295/60R22.5, 295/80R22.5 and 315/80R22.5 it was used an *unbalance ratio* equal to 0,25 (25% higher contact pressure for one wheel and 25% lower contact pressure for the other wheel).

From the results of the calculations it is proposed the following formula to take into account the effect of the unequal load sharing:

$$WEAR_{unbalanced\ load} = f_{load\ unbalance} \times WEAR_{balanced\ load}$$

Where:

$$f_{load\ unbalance} = 1 + \textit{unbalance ratio}$$

4.2 - Dual tyres versus wide single tyres

To allow a general comparison between dual (dashed lines) and wide single tyres (fill lines), Figures 5 and 6 present the rate of practical permanent deformation for all structures, respectively without and with the effect of lateral wandering.

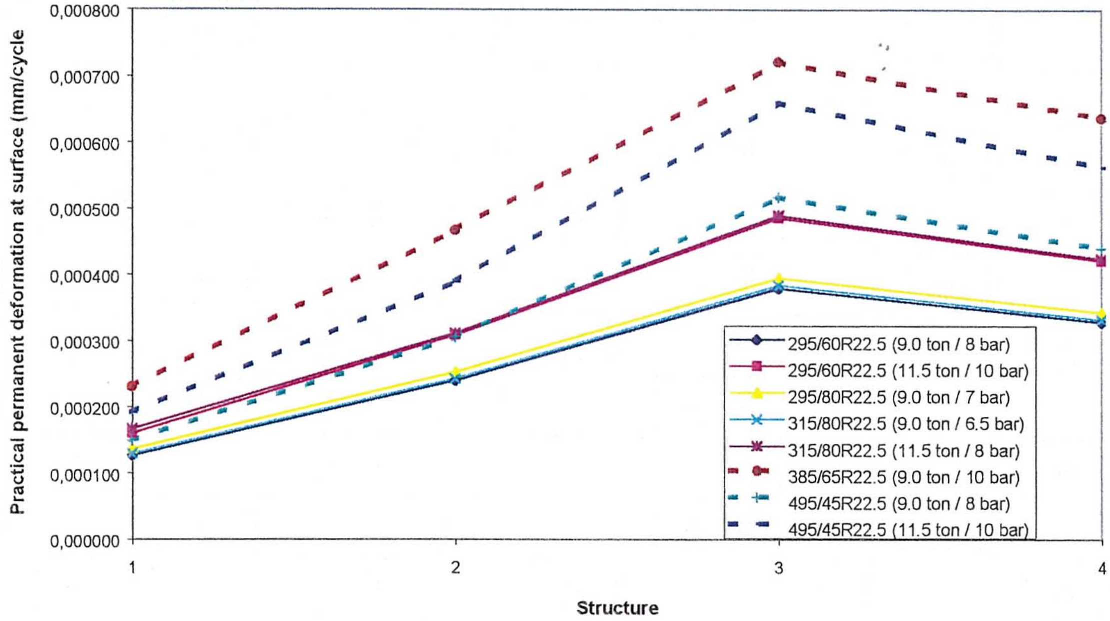

Figure 5 – Practical permanent deformation by cycle at surface, without the effect of lateral wandering, for different tyres and structures

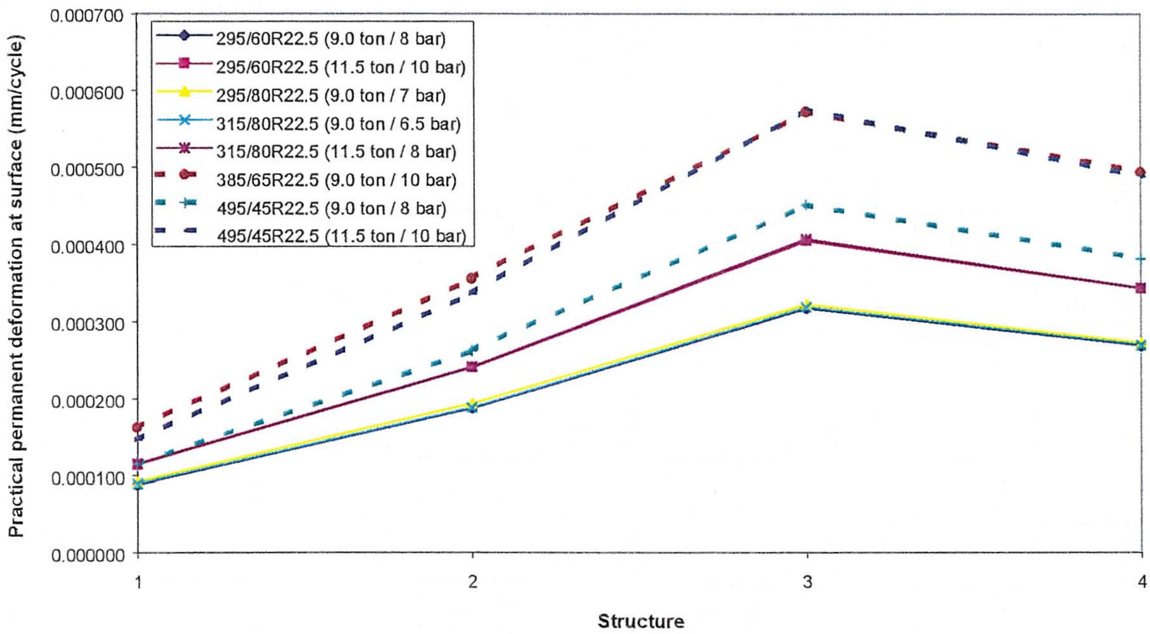

Figure 6 – Practical permanent deformation by cycle at surface, with the effect of lateral wandering, for different tyres and structures

The results presented in Figures 4 and 5 show that to the wide single tyres correspond the higher values of permanent deformation. The rating for wide single tyres from the more to the less aggressive tyre is: 385/65R22.5 (9.0 ton / 10 bar), 495/45R22.5 (11.5 ton / 10 bar) and 495/45R22.5 (9.0 ton / 8 bar). Therefore the 495/45R22.5 (11.5 ton / 10 bar), though with a higher load is less aggressive than the 385/65R22.5 (9.0 ton / 10 bar), which leads to the conclusion that it is necessary to consider the specific characteristics of the tyre to establish a relative effect between tyres (shape of contact area, tyre diameter and overinflation).

It is also interesting to note that the reduction of permanent deformation with the effect of the lateral wandering is more pronounced for the 385/65R22.5 (9.0 ton / 10 bar) and for the dual tyres.

4.3 - Tyre inflation pressure and size of the contact area

The characteristics of the tyres considered in the calculations were the inflation pressure and the total load. In fact the effect of loading is connected to a contact pressure, where the ratio to the inflation pressure is not the same for different tyres, taking values in the range of 64% - 79% for the tyres considered in the calculations. It was also assumed a constant pressure over all the contact area. So the pressure used in the calculations is, in fact, an average contact pressure.

An analysis of the results has showed that the effect of tyre loads in terms of primary rutting was related to the shape of the contact area. Table 8 illustrates this effect, considering the same load, but different shapes for the contact area (square, and length/width=0.64, length/width=1.56 and length/width=0.80).

Table 8 – Parametric study

Tyre	Load (kN)	Width (mm)	Length (mm)	Contact area (mm^2)	Contact pressure (kNm^{-2})	Rate of permanent deformation (mm/cycle)
A	28.75	180	180	32400	887.3	0.000837
B		144	225	32400	887.3	0.001011
C		225	144	32400	887.3	0.000675
D		144	180	25920	1109.2	0.001011

Asphalt layer thickness=300 mm
Serial damper=3000 MNm^{-2}s
Speed=11.11ms^{-1} (40km/h)
Poisson's ratio=0.40

These calculations show that the permanent deformation for tyre B and tyre D (equal load, different contact pressure and equal contact area width) is equal. It can also be seen that higher values of the contact area width correspond lower values of the permanent deformation (tyres A, B and C).

Figure 7 presents the relationship between practical permanent deformation, thickness and load configuration for different tyres and structures to take into account all these factors. Though a better correlation was obtained when the effect of lateral wandering was not considered, it is also acceptable for the results with the effect of lateral wandering.

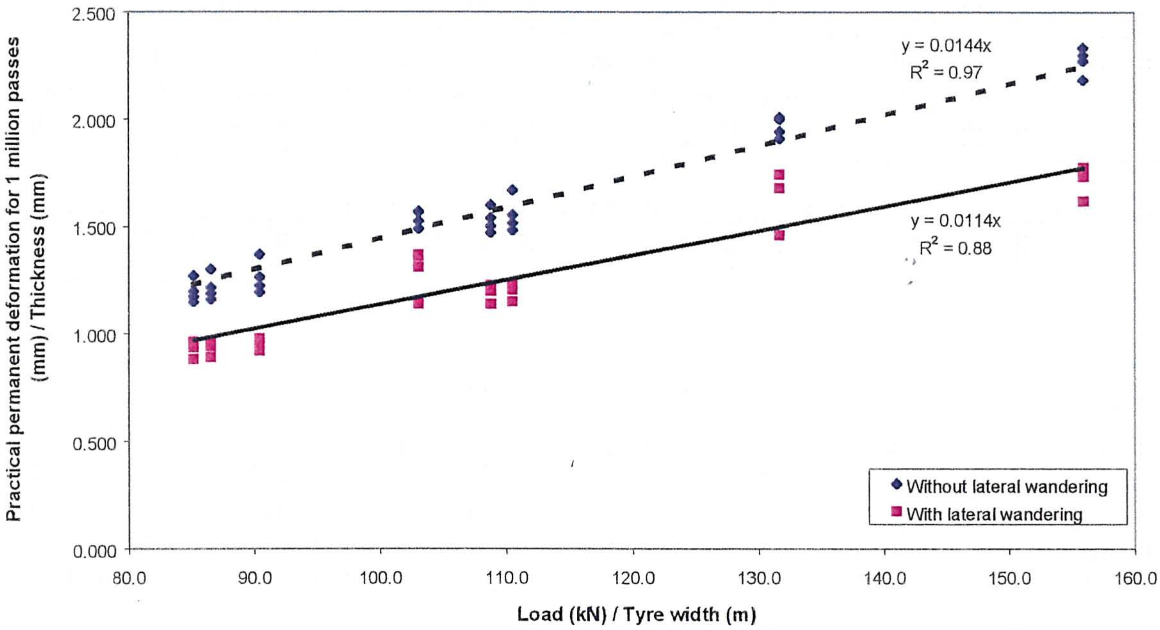

Figure 7 – Relation between practical permanent deformation, thickness and load configuration for different tyres and structures

These results lead to the following formula for the factor that considers the configuration of the tyre:

$$f_{configuration\ tyre} = \frac{\dfrac{P \times h}{w}}{\left[\dfrac{P \times h}{w}\right]_{ref}}$$

Where P is the axle load (kN), h is the total asphalt layer thickness (m) and w is the total tyre width (m) – the sum of the width of both tyres for duals.

If the reference tyre is the 315/80R22.5 (11.5 ton / 8 bar) the factor for configuration of the tyre assumes the following formula:

$$f_{configuration\ tyre} = \frac{h}{44} \times \frac{P}{w}$$

From the calculations it is proposed the following formula to take into account the effect of the tyre inflation pressure and size and shape of the contact area:

$$\text{WEAR} = f_{\text{configuration tyre}} \times \text{WEAR}_{\text{reference tyre}}$$

5 - FINAL REMARKS

From the results of the research the effect on primary rutting of the unequal load sharing, the magnitude of the inflation pressure and the size of contact area for both dual and wide single tyres was expressed mathematically as follows:

Dual Tyres versus Wide Single Tyre:

The results presented show that to the wide single tyres correspond the higher values of permanent deformation. The results show that the dual tyres with a total axle load of 11,5 tonnes (5750 kg per dual tyre assembly or 2875 kg per tyre) are less aggressive than the single tyres with a total axle load of 9,0 tonnes (4500 kg per tyre).

The ranking of the tyres at equal load and with the same inflation pressure is qualitatively as follows (from the less to the more aggressive tyre): dual tyre 295/60R22.5, dual tyre 315/80R22.5, dual tyre 295/80R22.5, extra wide single tyre 495/45R22.5 and wide single tyre 385/65R22.5. These dual tyres have similar effect on the permanent deformation of bituminous layers.

Unequal load sharing:

$$WEAR_{unbalanced\ load} = f_{load\ unbalance} \times WEAR_{balanced\ load}$$

Where:

$$f_{load\ unbalance} = 1 + \textit{unbalance ratio}$$

Tyre inflation pressure and size of the contact area:

$$WEAR = f_{configuration\ tyre} \times WEAR_{reference\ tyre}$$

Laboratório Nacional de Engenharia Civil. Lisbon, June 2000

SEEN

The Head of Pavements Division

Luís Quaresma

The Head of Transportation

António Pinelo

The Head of Experimental design
and Special Studies Division

Carlos Brito Pina

The Head of Dams Department

João Castel-Branco Falcão

AUTHORS

Luís Quaresma
Senior Research Officer

Pedro Salvado Ferreira
Civil Engineer

António Lopes Batista
Research Officer

6 - REFERENCES

Batista, A. L. - *Análise do comportamento ao longo do tempo de barragens abóbada*, Phd Thesis - Universidade Técnica de Lisboa. Instituto Superior Técnico, 1998.

Metcalfe, Andrew V. - *Statistics in Civil Engineering* – Arnold Applications of Statistics Series,1997.

Penant, Christophe – Information about tyre footprint data – Michelin, 1999.

Quaresma, Luís; Ferreira, Pedro S.; Freire, Ana C. and Batista, António L. - *Mechanistic approach for rutting - Stage 1* – LNEC, 2000.

Quaresma, Luís; Ferreira, Pedro S. and Freire, Ana C. - *Mechanistic approach for rutting - Stage 2* – LNEC, 2000.

APPENDIX

Results from CREEPN

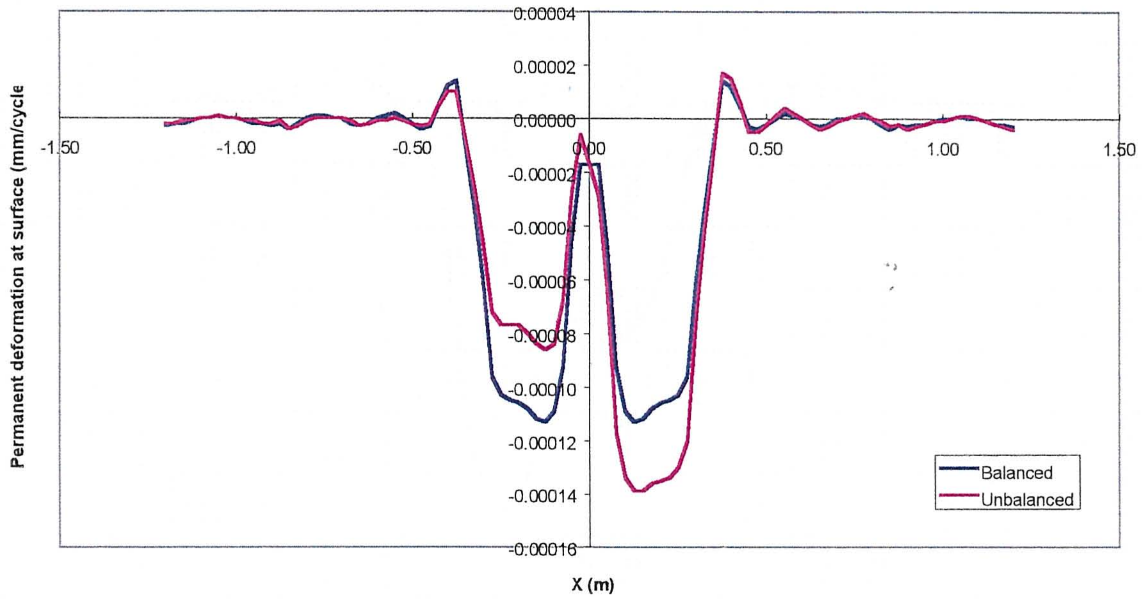

Figure A.1 – Permanent deformation by cycle at surface for the tyre 295/60R22.5 (9.0 ton / 8 bar) with balanced and unbalanced load in pavement 1 without the effect of the lateral wandering

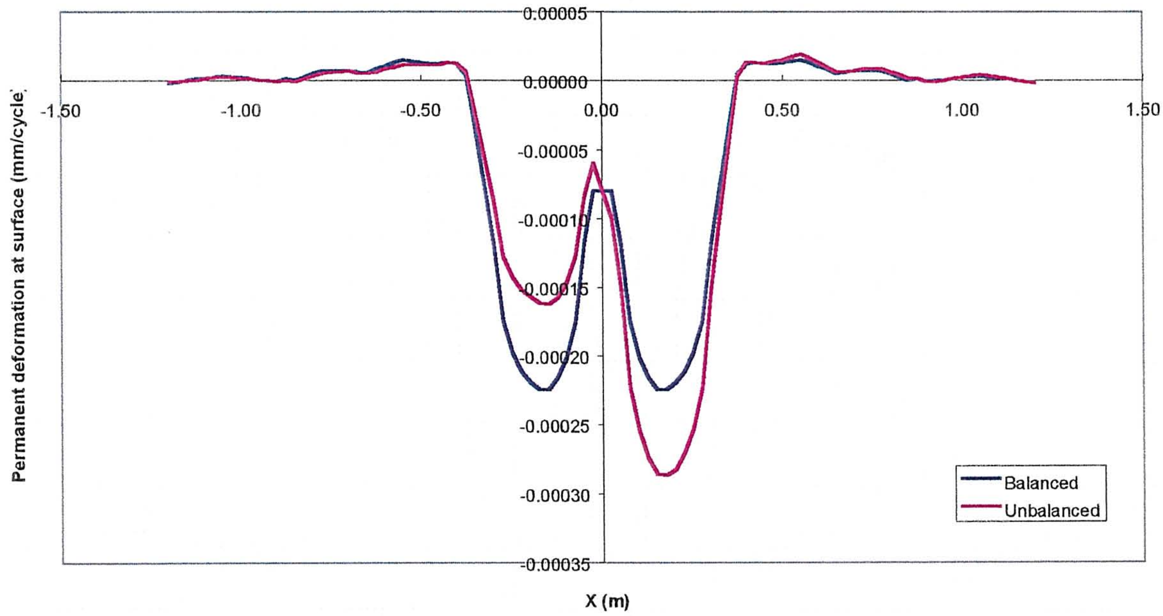

Figure A.2 – Permanent deformation by cycle at surface for the tyre 295/60R22.5 (9.0 ton / 8 bar) with balanced and unbalanced load in pavement 2 without the effect of the lateral wandering

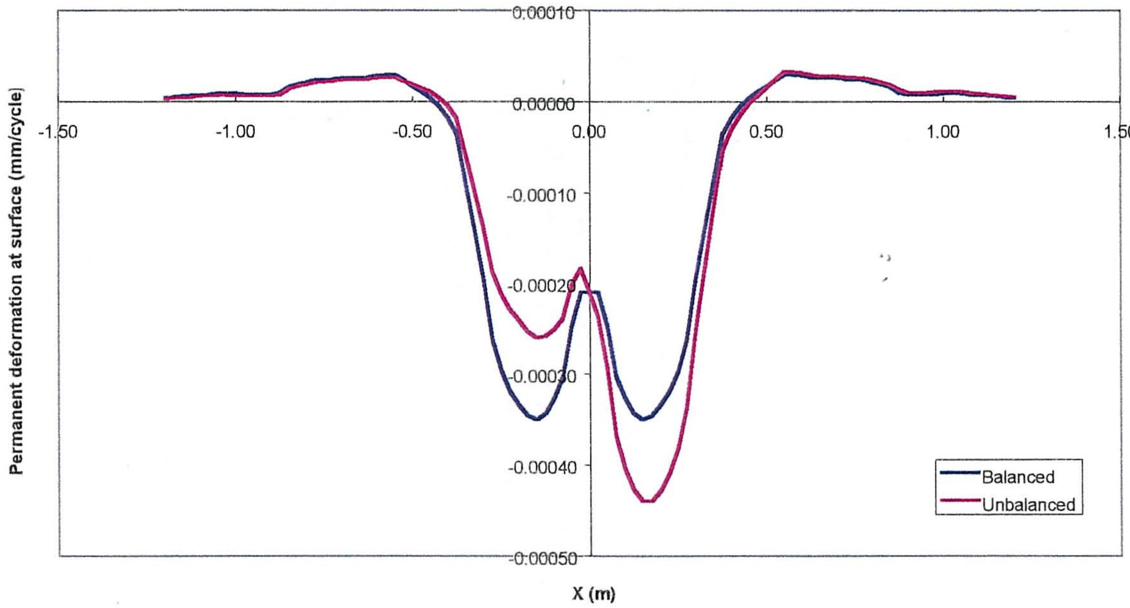

Figure A.3 – Permanent deformation by cycle at surface for the tyre 295/60R22.5 (9.0 ton / 8 bar) with balanced and unbalanced load in pavement 3 without the effect of the lateral wandering

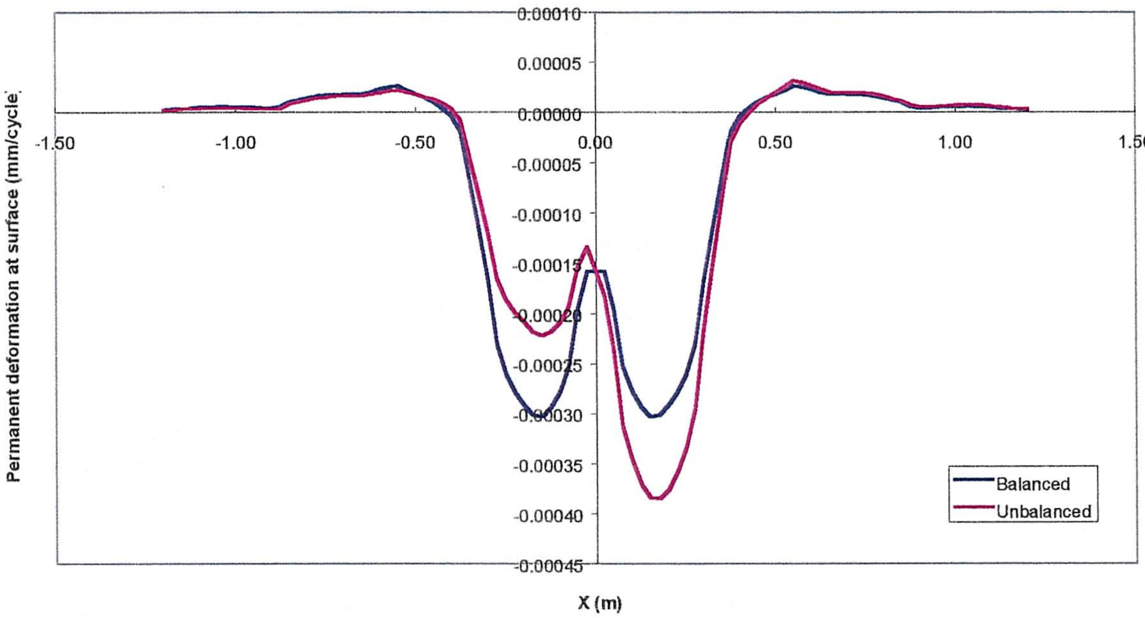

Figure A.4 – Permanent deformation by cycle at surface for the tyre 295/60R22.5 (9.0 ton / 8 bar) with balanced and unbalanced load in pavement 4 without the effect of the lateral wandering

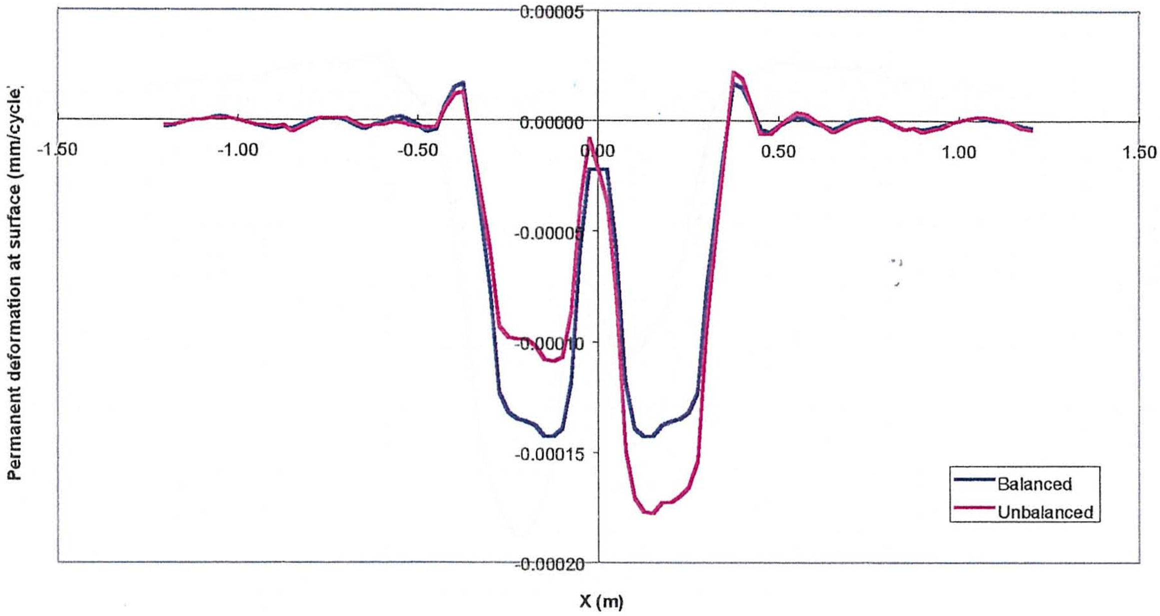

Figure A.5 – Permanent deformation by cycle at surface for the tyre 295/60R22.5 (11.5 ton / 10 bar) with balanced and unbalanced load in pavement 1 without the effect of the lateral wandering

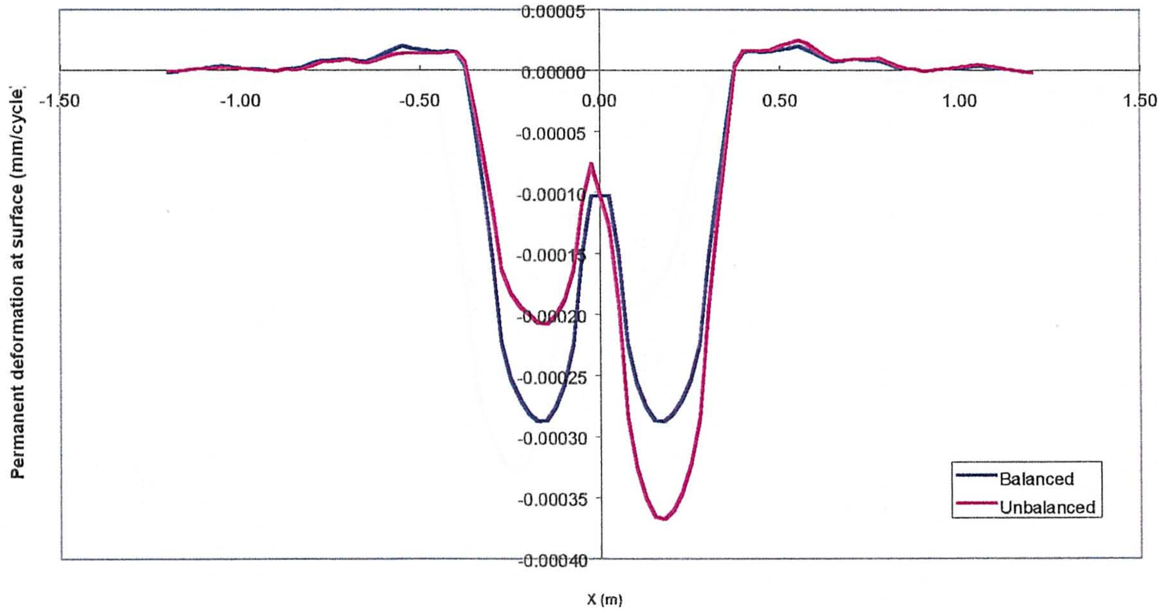

Figure A.6 – Permanent deformation by cycle at surface for the tyre 295/60R22.5 (11.5 ton / 10 bar) with balanced and unbalanced load in pavement 2 without the effect of the lateral wandering

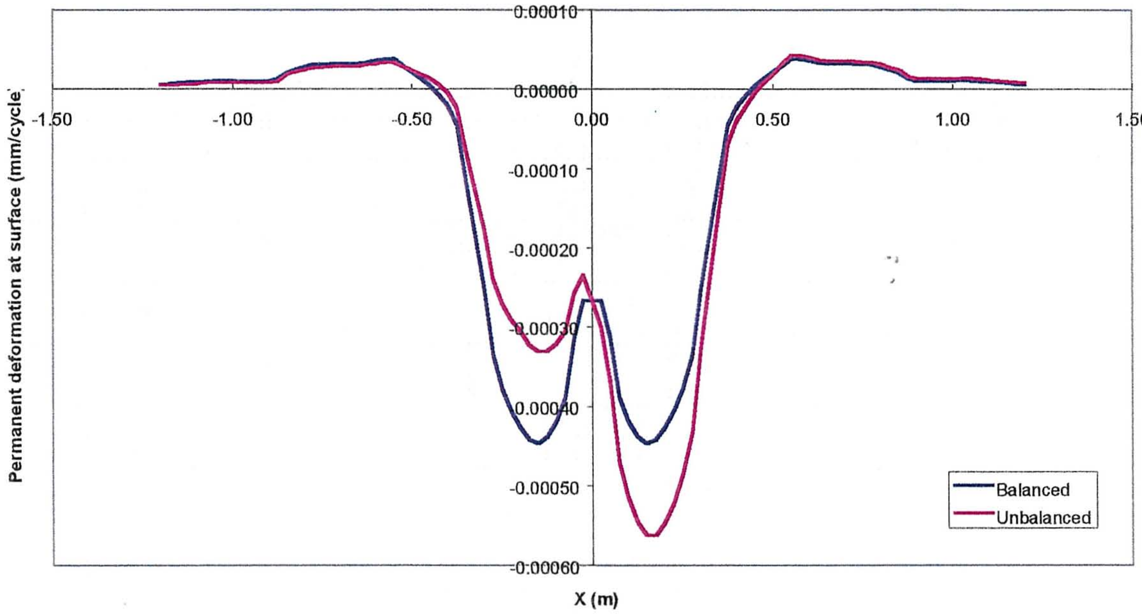

Figure A.7 – Permanent deformation by cycle at surface for the tyre 295/60R22.5 (11.5 ton / 10 bar) with balanced and unbalanced load in pavement 3 without the effect of the lateral wandering

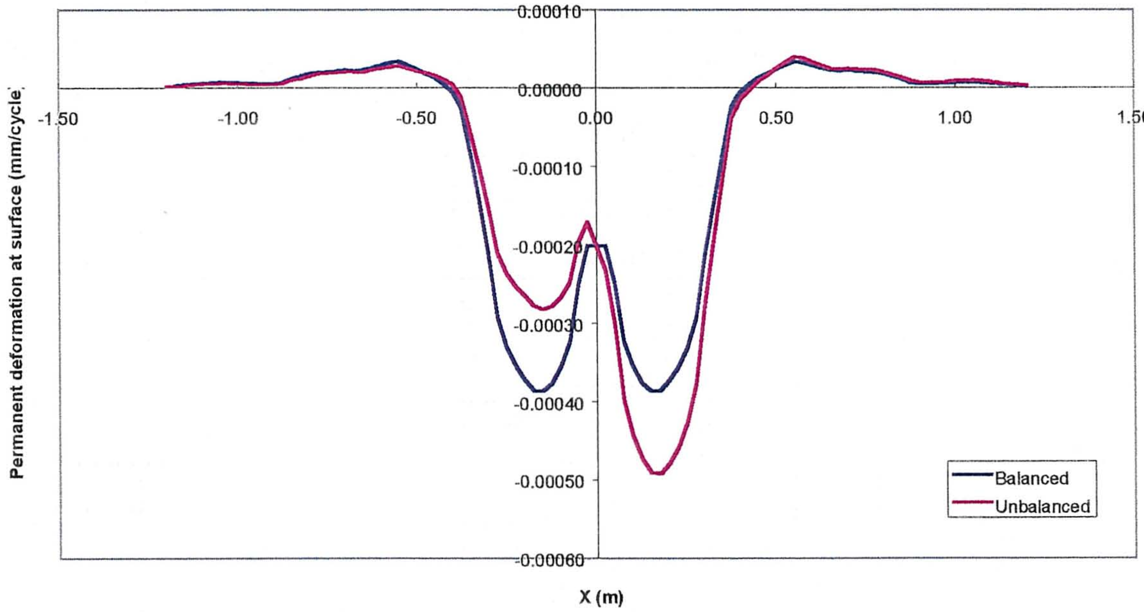

Figure A.8 – Permanent deformation by cycle at surface for the tyre 295/60R22.5 (11.5 ton / 10 bar) with balanced and unbalanced load in pavement 4 without the effect of the lateral wandering

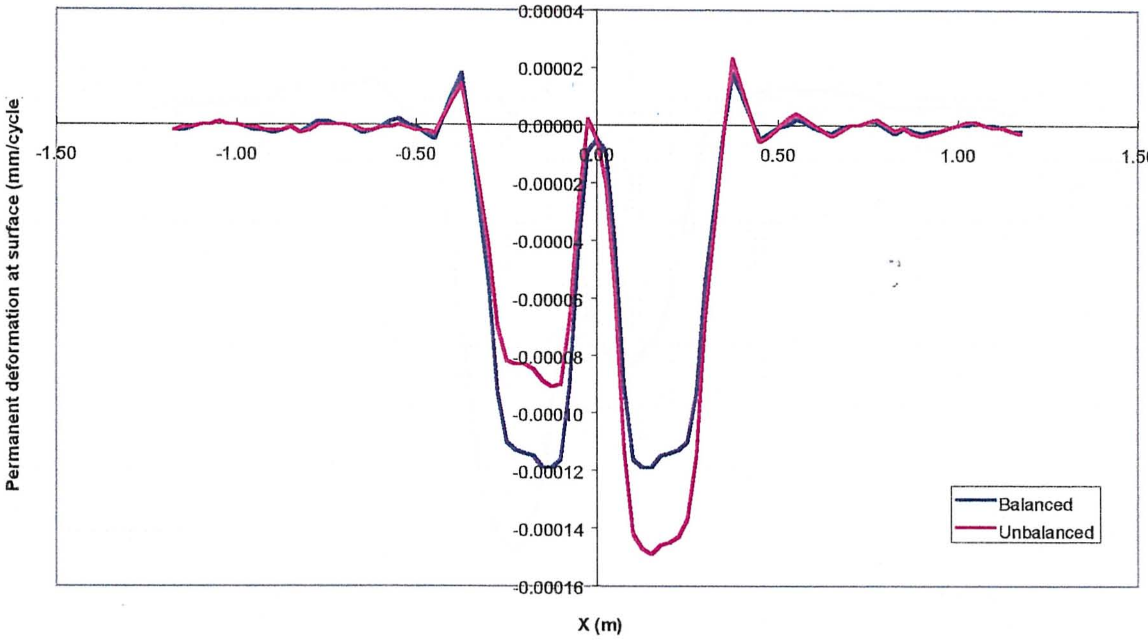

Figure A.9 – Permanent deformation by cycle at surface for the tyre 295/80R22.5 (9.0 ton / 7 bar) with balanced and unbalanced load in pavement 1 without the effect of the lateral wandering

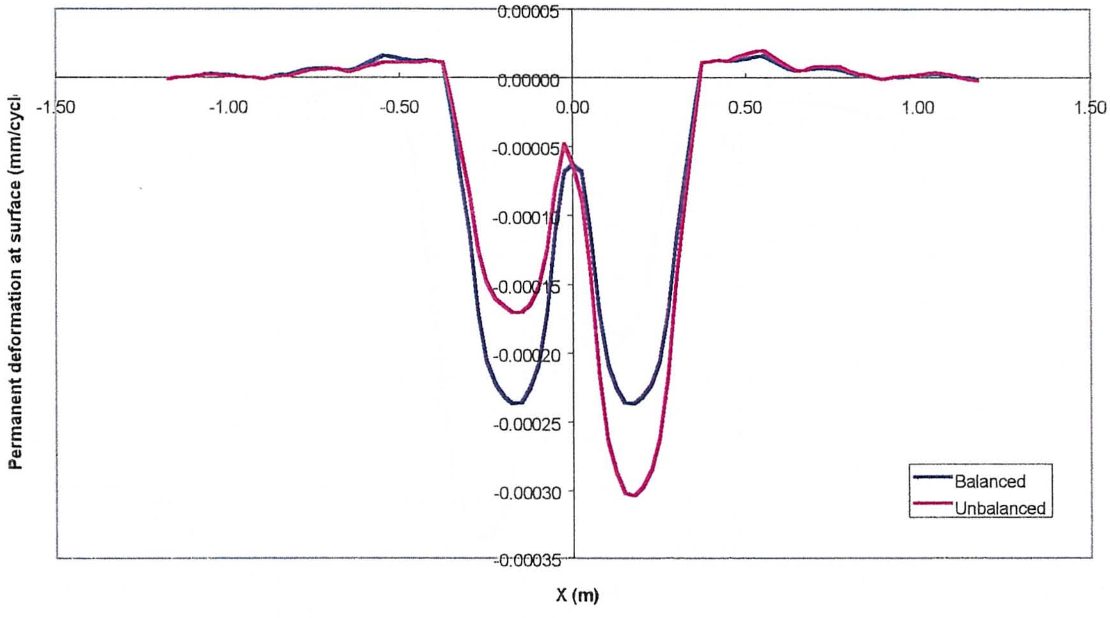

Figure A.10 – Permanent deformation by cycle at surface for the tyre 295/80R22.5 (9.0 ton / 7 bar) with balanced and unbalanced load in pavement 2 without the effect of the lateral wandering

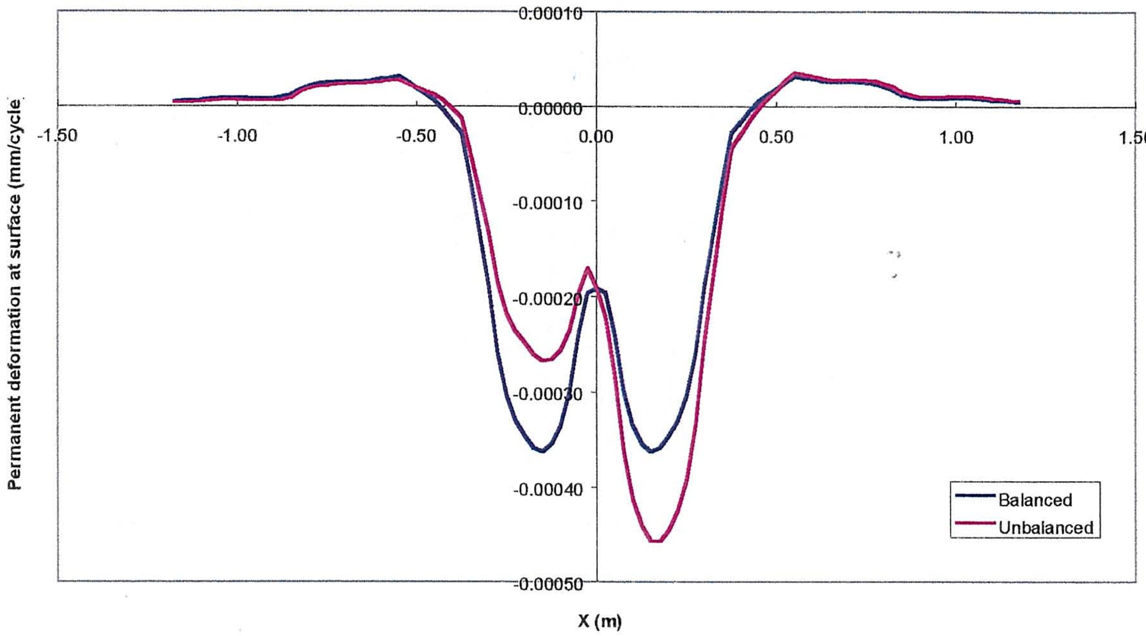

Figure A.11 – Permanent deformation by cycle at surface for the tyre 295/80R22.5 (9.0 ton / 7 bar) with balanced and unbalanced load in pavement 3 without the effect of the lateral wandering

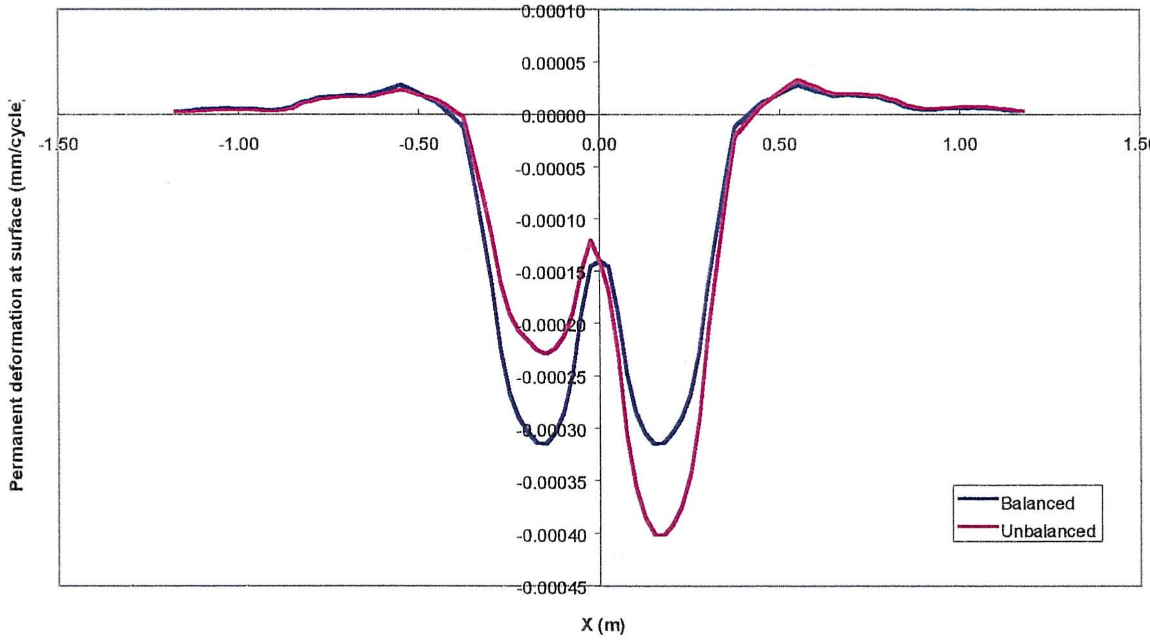

Figure A.12 – Permanent deformation by cycle at surface for the tyre 295/80R22.5 (9.0 ton / 7 bar) with balanced and unbalanced load in pavement 4 without the effect of the lateral wandering

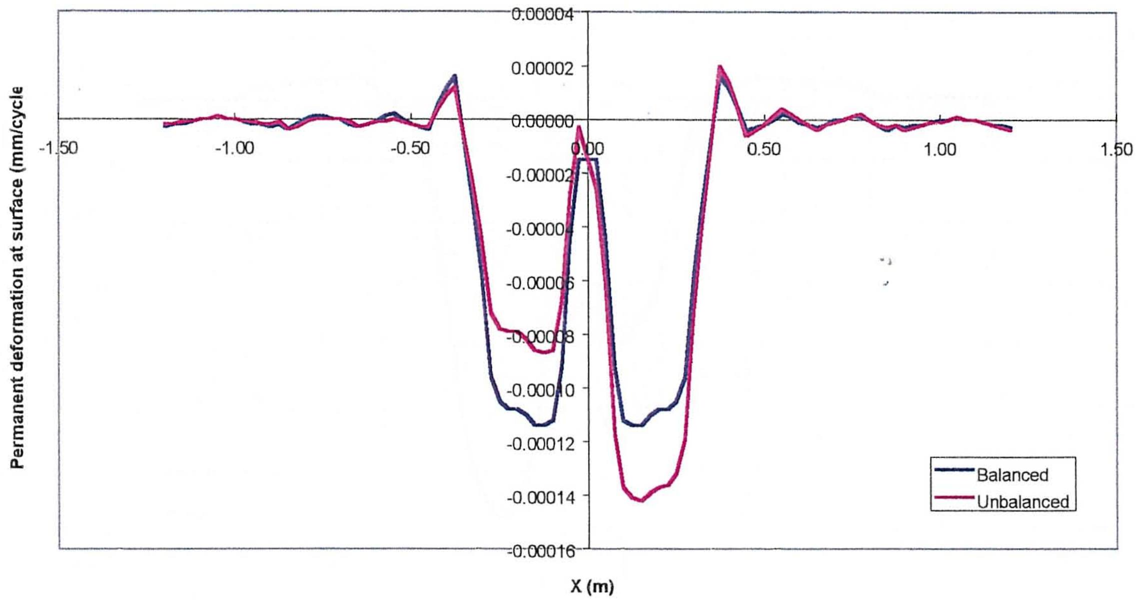

Figure A.13 – Permanent deformation by cycle at surface for the tyre 315/80R22.5 (9.0 ton / 6.5 bar) with balanced and unbalanced load in pavement 1 without the effect of the lateral wandering

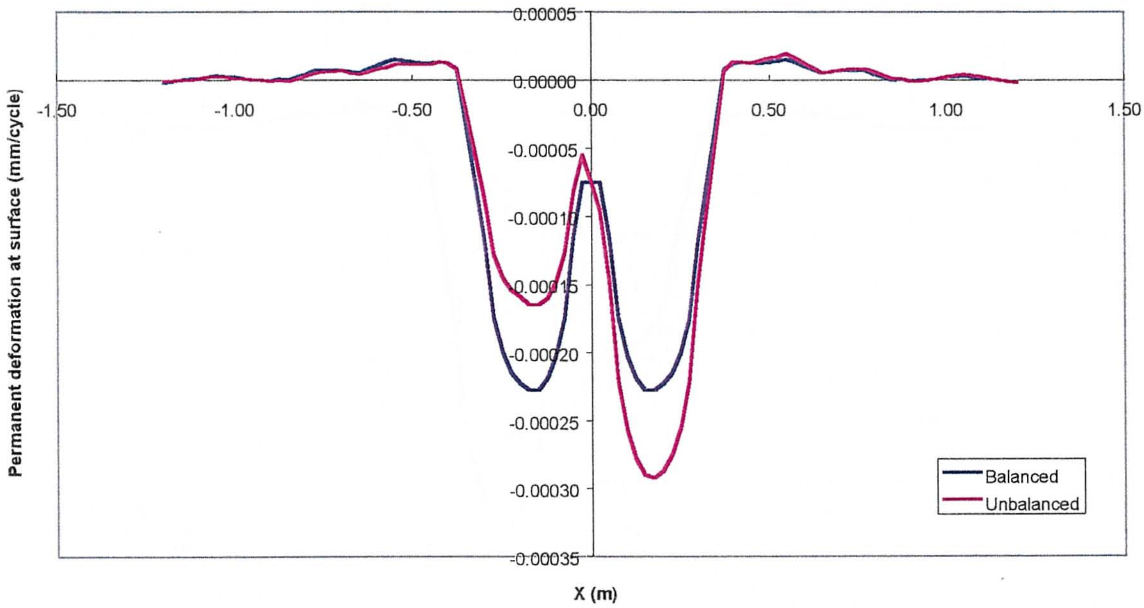

Figure A.14 – Permanent deformation by cycle at surface for the tyre 315/80R22.5 (9.0 ton / 6.5 bar) with balanced and unbalanced load in pavement 2 without the effect of the lateral wandering

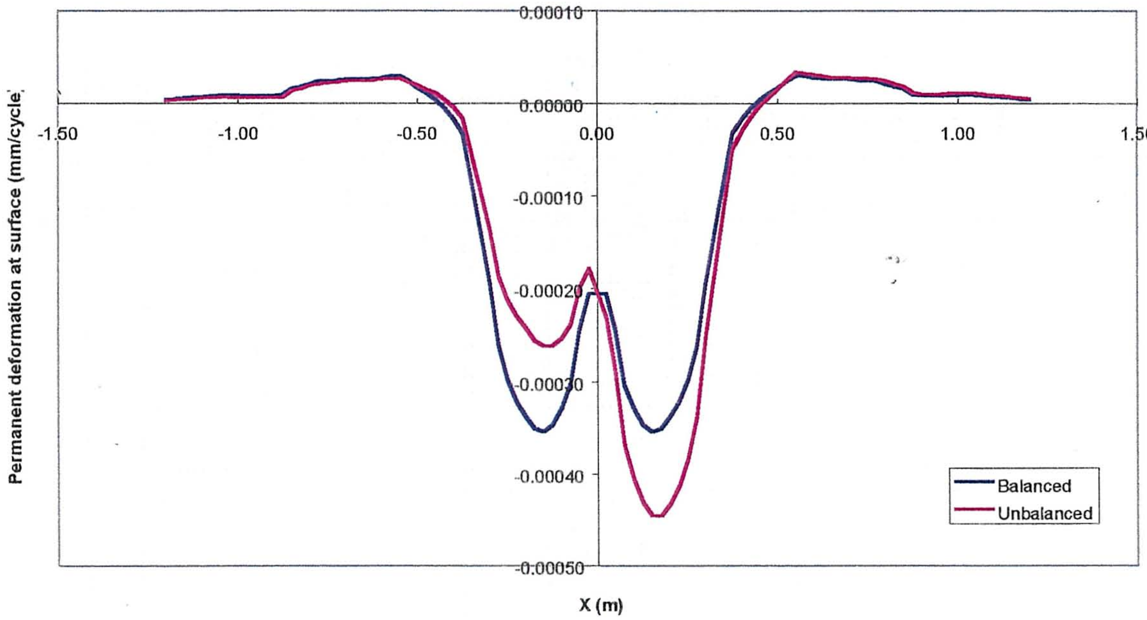

Figure A.15 – Permanent deformation by cycle at surface for the tyre 315/80R22.5 (9.0 ton / 6.5 bar) with balanced and unbalanced load in pavement 3 without the effect of the lateral wandering

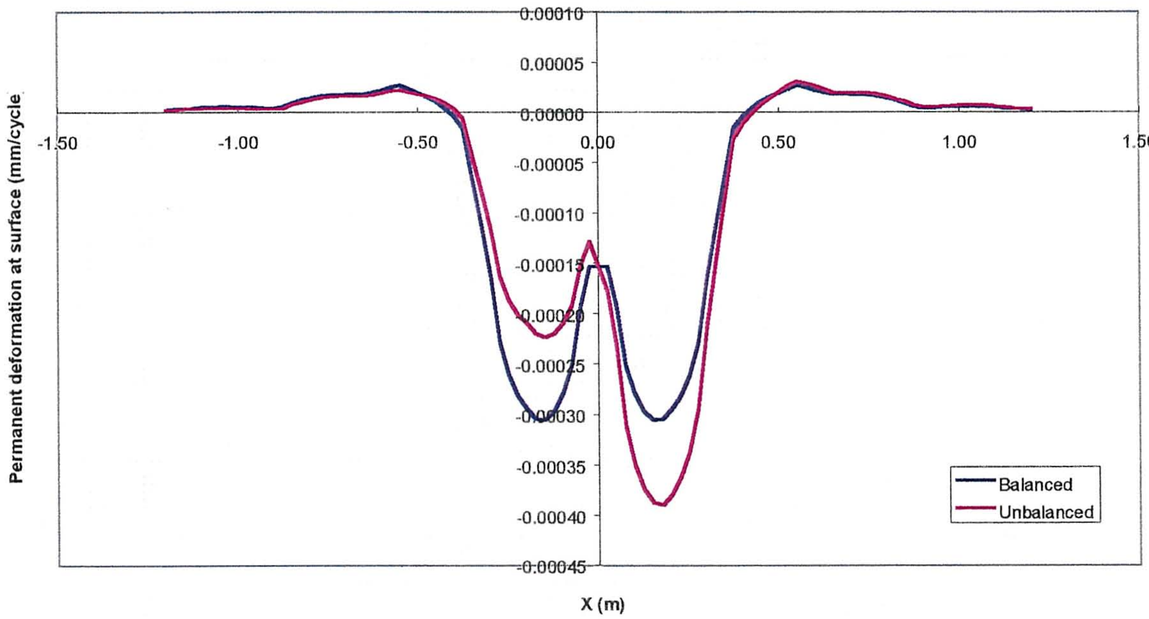

Figure A.16 – Permanent deformation by cycle at surface for the tyre 315/80R22.5 (9.0 ton / 6.5 bar) with balanced and unbalanced load in pavement 4 without the effect of the lateral wandering

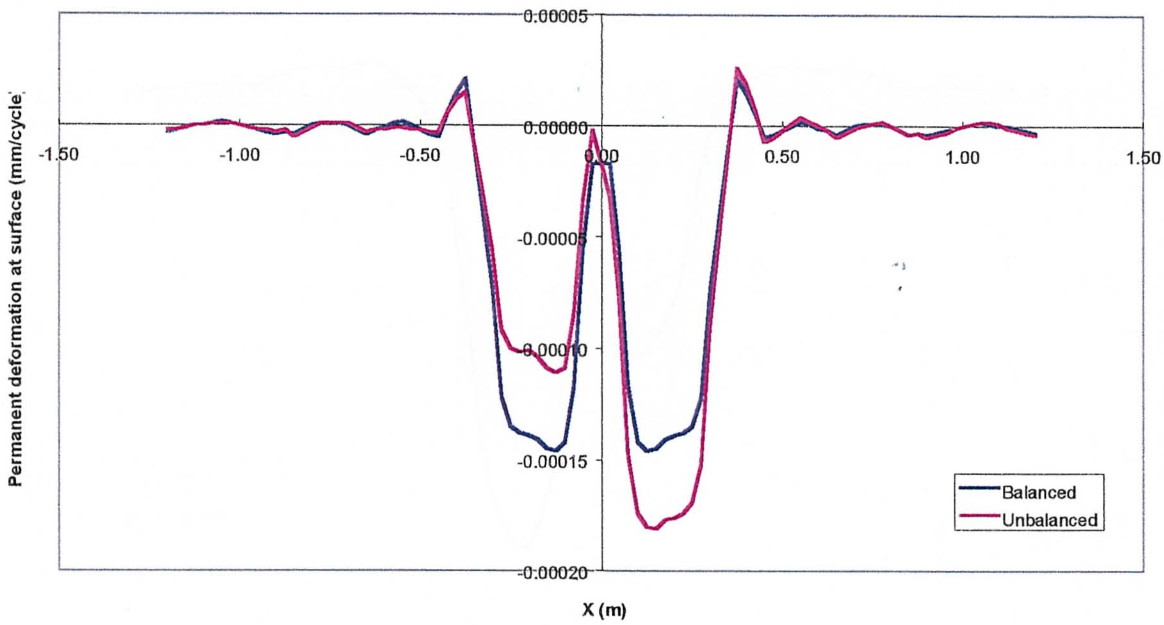

Figure A.17 – Permanent deformation by cycle at surface for the tyre 315/80R22.5 (11.5 ton / 8 bar) with balanced and unbalanced load in pavement 1 without the effect of the lateral wandering

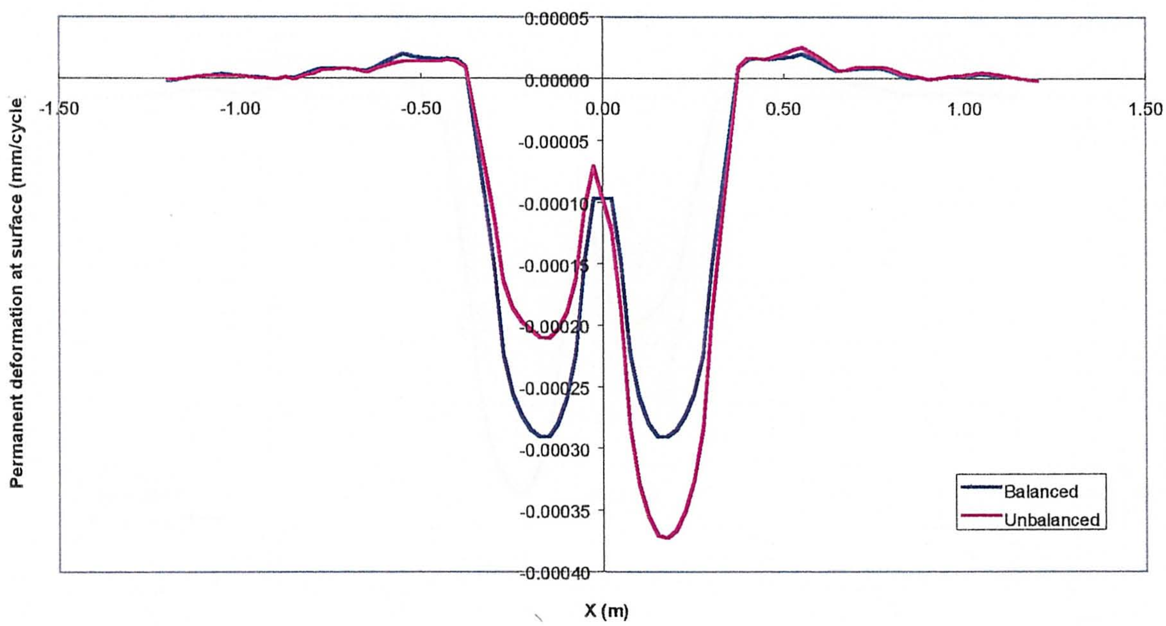

Figure A.18 – Permanent deformation by cycle at surface for the tyre 315/80R22.5 (11.5 ton / 8 bar) with balanced and unbalanced load in pavement 2 without the effect of the lateral wandering

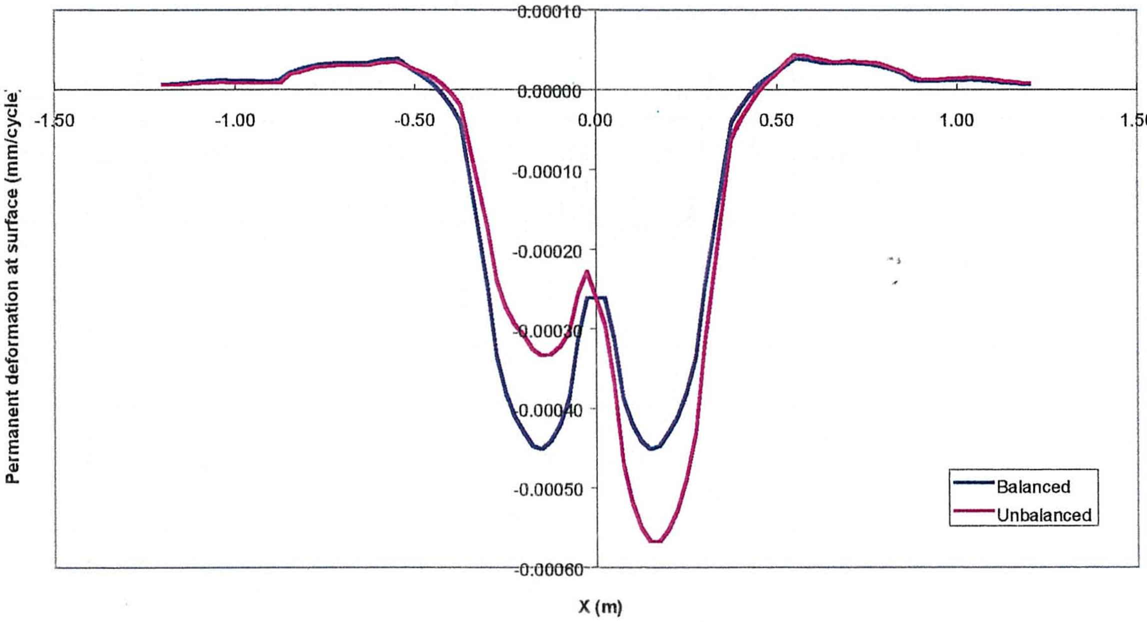

Figure A.19 – Permanent deformation by cycle at surface for the tyre 315/80R22.5 (11.5 ton / 8 bar) with balanced and unbalanced load in pavement 3 without the effect of the lateral wandering

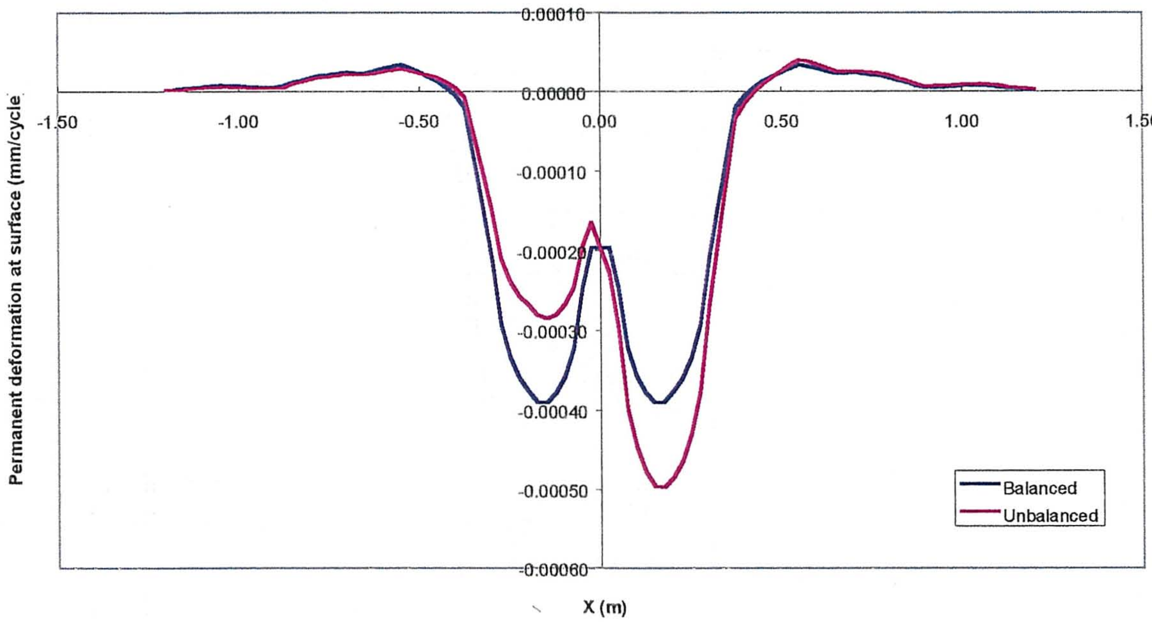

Figure A.20 – Permanent deformation by cycle at surface for the tyre 315/80R22.5 (11.5 ton / 8 bar) with balanced and unbalanced load in pavement 4 without the effect of the lateral wandering

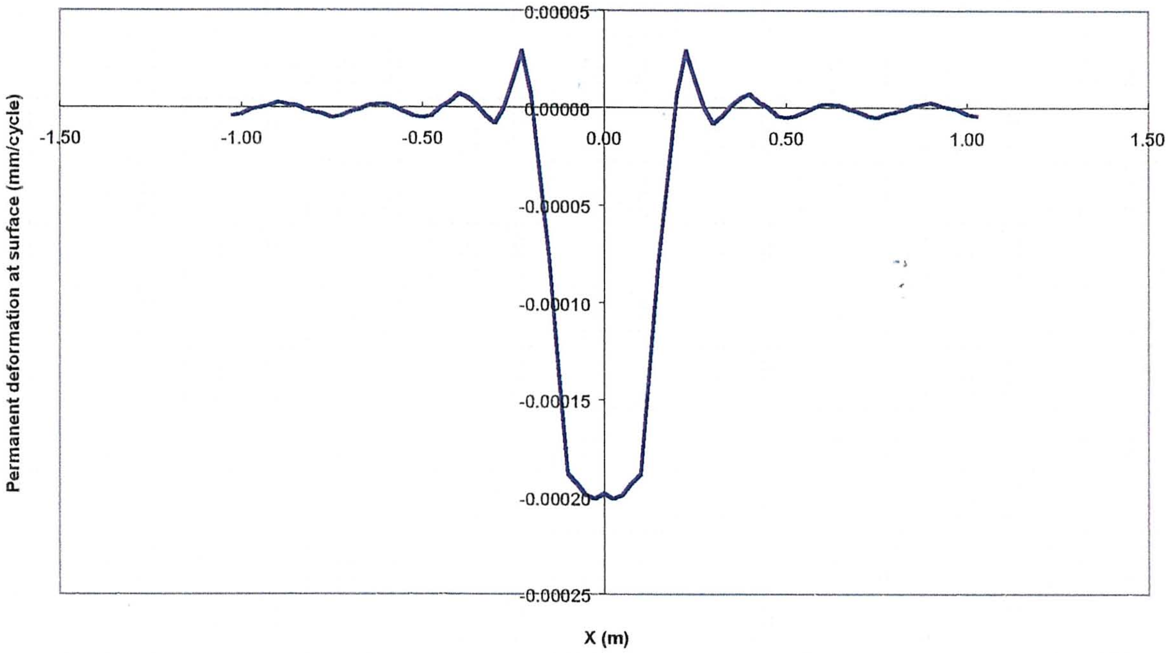

Figure A.21 – Permanent deformation by cycle at surface for the tyre 385/65R22.5 (9.0 ton / 10 bar) in pavement 1 without the effect of the lateral wandering

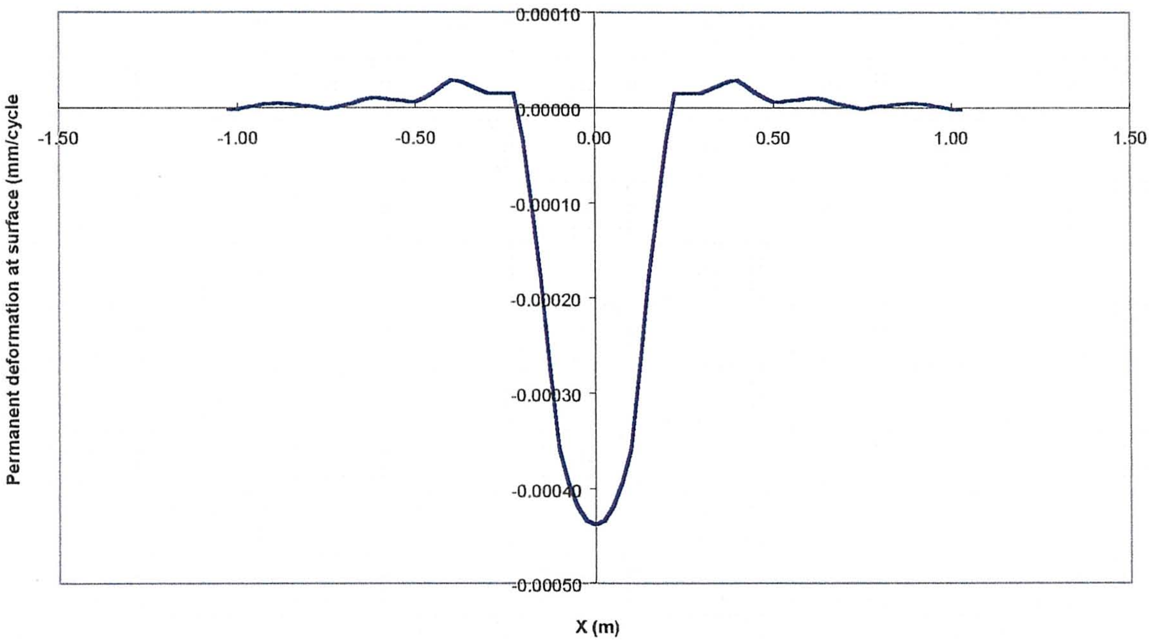

Figure A.22 – Permanent deformation by cycle at surface for the tyre 385/65R22.5 (9.0 ton / 10 bar) in pavement 2 without the effect of the lateral wandering

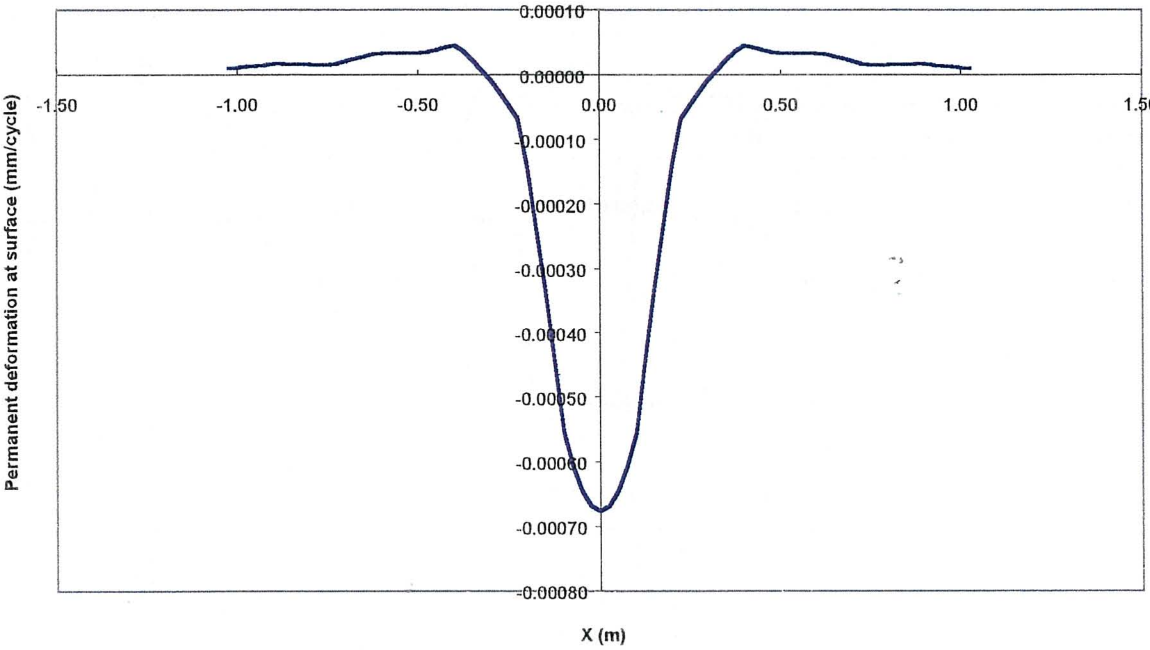

Figure A.23 – Permanent deformation by cycle at surface for the tyre 385/65R22.5 (9.0 ton / 10 bar) in pavement 3 without the effect of the lateral wandering

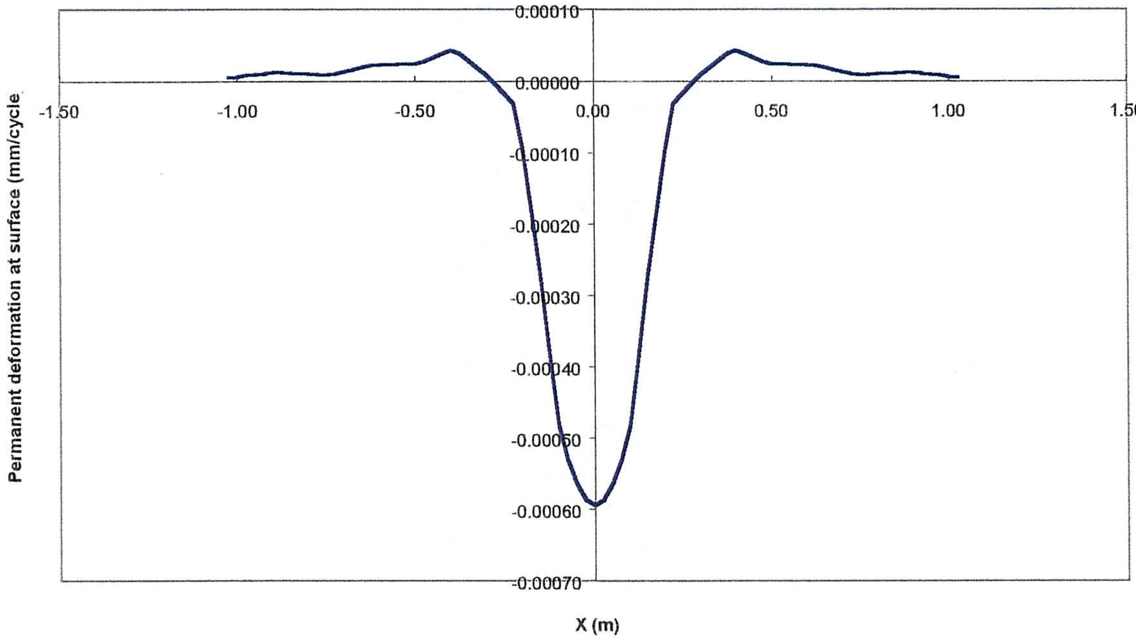

Figure A.24 – Permanent deformation by cycle at surface for the tyre 385/65R22.5 (9.0 ton / 10 bar) in pavement 4 without the effect of the lateral wandering

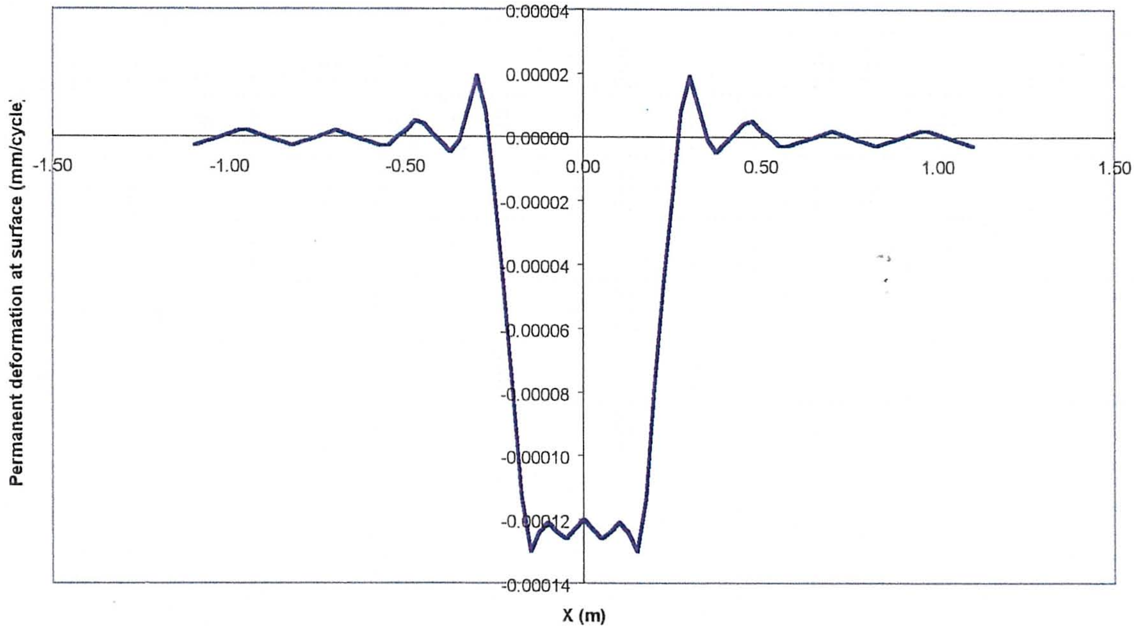

Figure A.25 – Permanent deformation by cycle at surface for the tyre 495/45R22.5 (9.0 ton / 8 bar) in pavement 1 without the effect of the lateral wandering

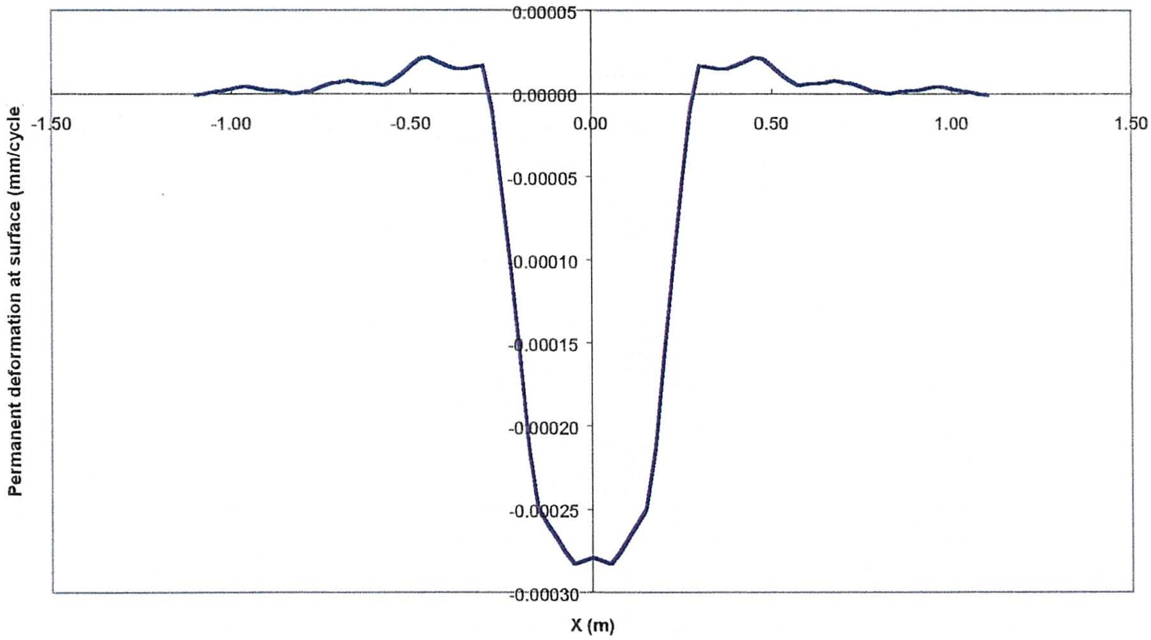

Figure A.26 – Permanent deformation by cycle at surface for the tyre 495/45R22.5 (9.0 ton / 8 bar) in pavement 2 without the effect of the lateral wandering

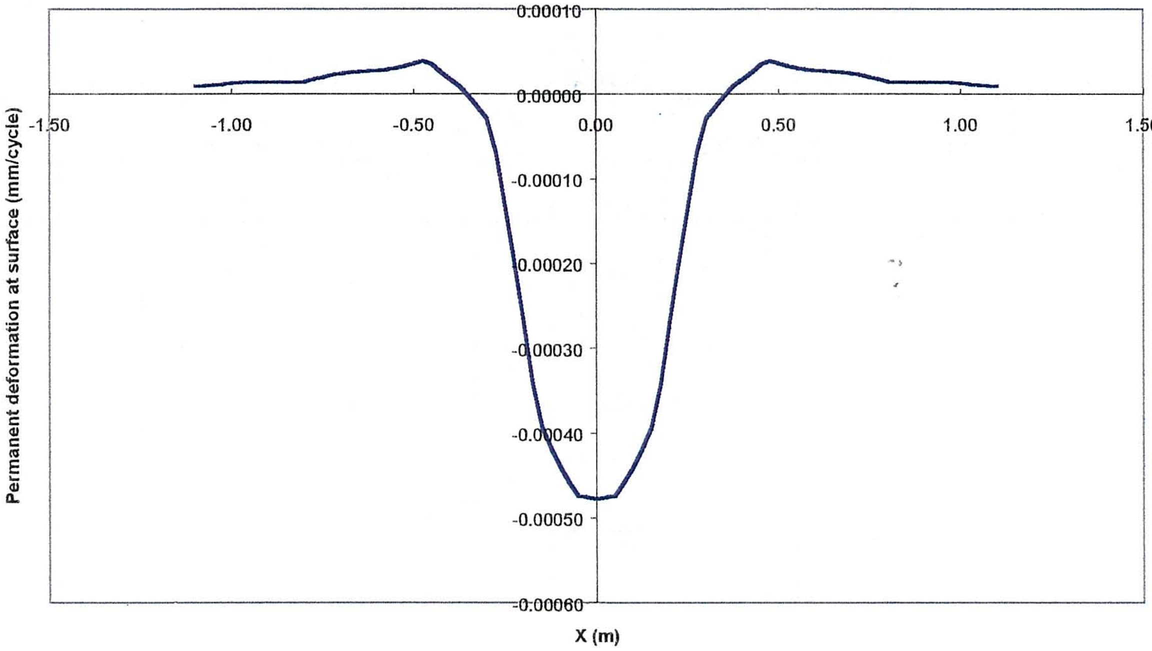

Figure A.27 – Permanent deformation by cycle at surface for the tyre 495/45R22.5 (9.0 ton / 8 bar) in pavement 3 without the effect of the lateral wandering

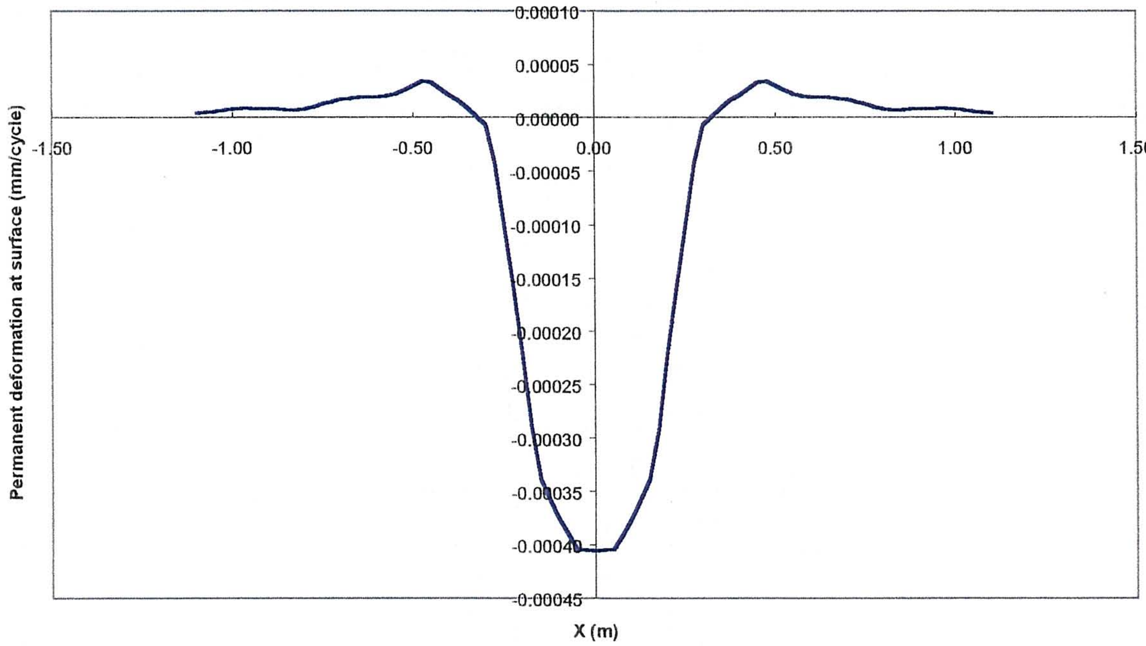

Figure A.28 – Permanent deformation by cycle at surface for the tyre 495/45R22.5 (9.0 ton / 8 bar) in pavement 4 without the effect of the lateral wandering

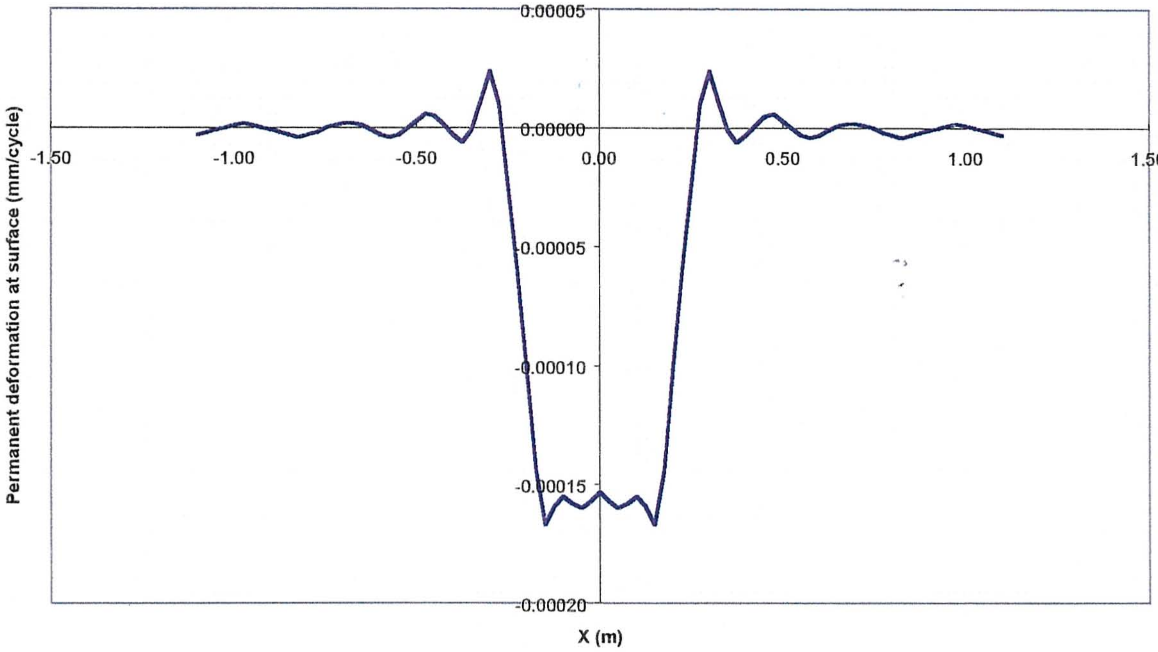

Figure A.29 – Permanent deformation by cycle at surface for the tyre 495/45R22.5 (11.5 ton / 10 bar) in pavement 1 without the effect of the lateral wandering

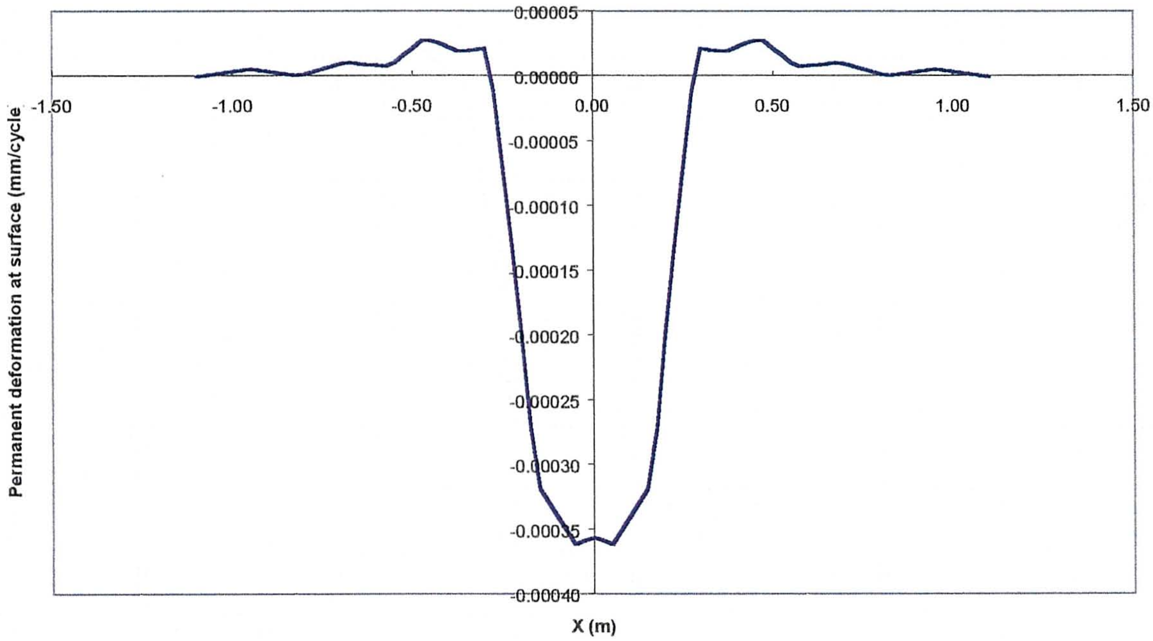

Figure A.30 – Permanent deformation by cycle at surface for the tyre 495/45R22.5 (11.5 ton / 10 bar) in pavement 2 without the effect of the lateral wandering

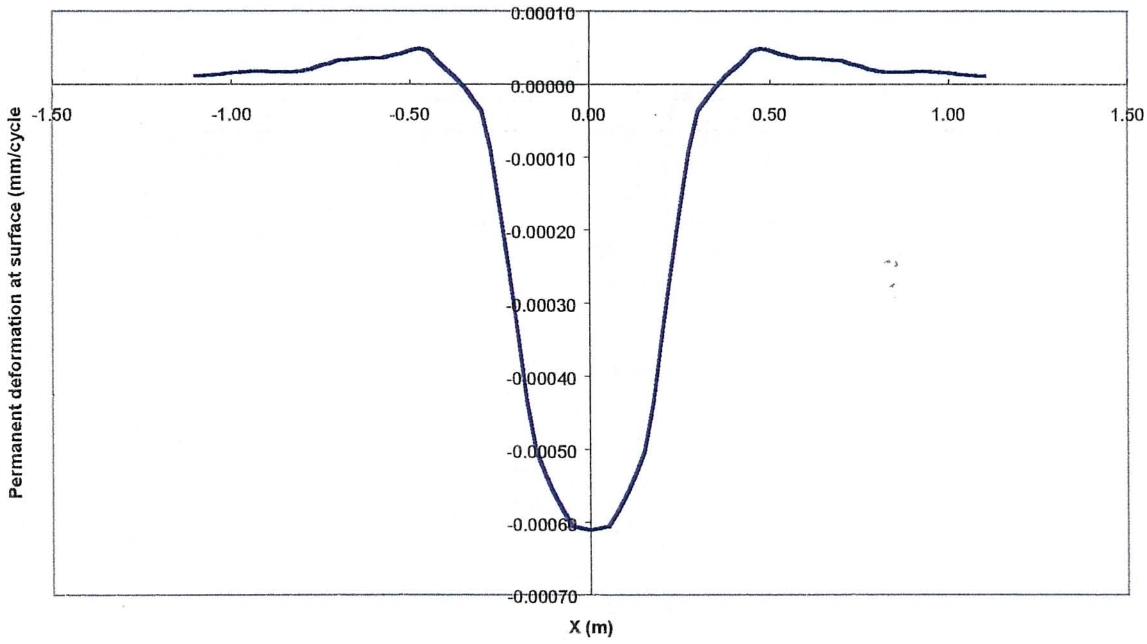

Figure A.31 – Permanent deformation by cycle at surface for the tyre 495/45R22.5 (11.5 ton / 10 bar) in pavement 3 without the effect of the lateral wandering

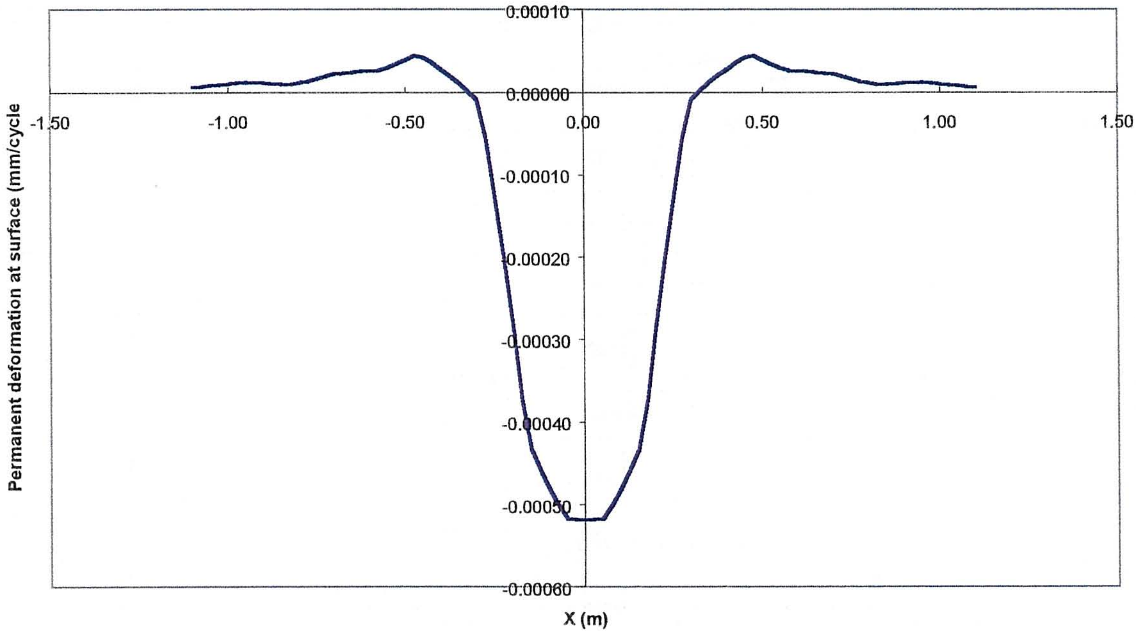

Figure A.32 – Permanent deformation by cycle at surface for the tyre 495/45R22.5 (11.5 ton / 10 bar) in pavement 4 without the effect of the lateral wandering

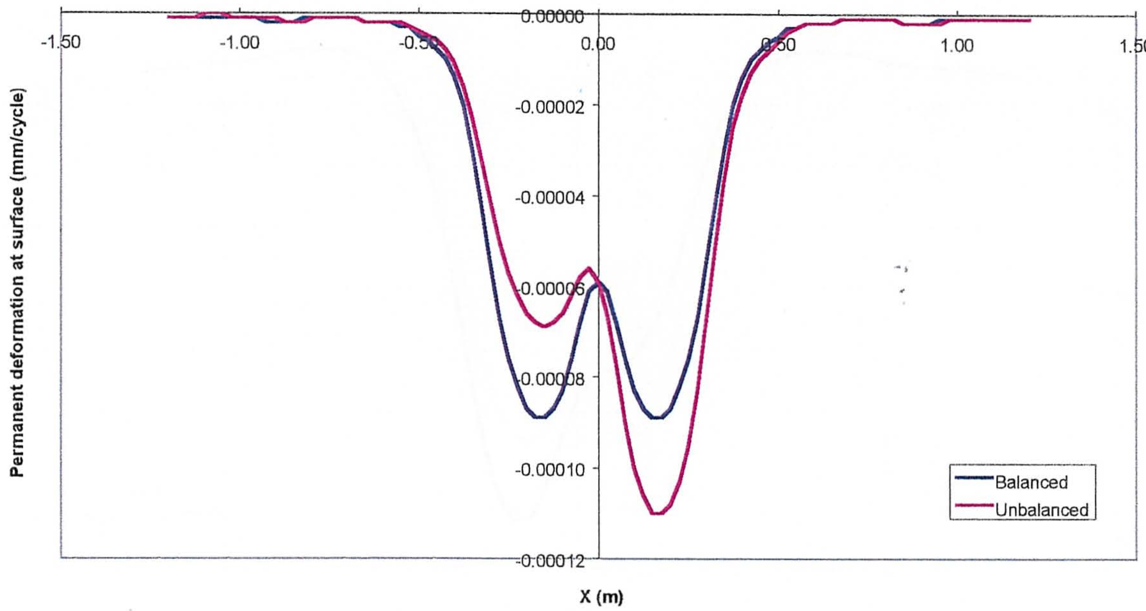

Figure A.33 – Permanent deformation by cycle at surface for the tyre 295/60R22.5 (9.0 ton / 8 bar) with balanced and unbalanced load in pavement 1 with the effect of the lateral wandering

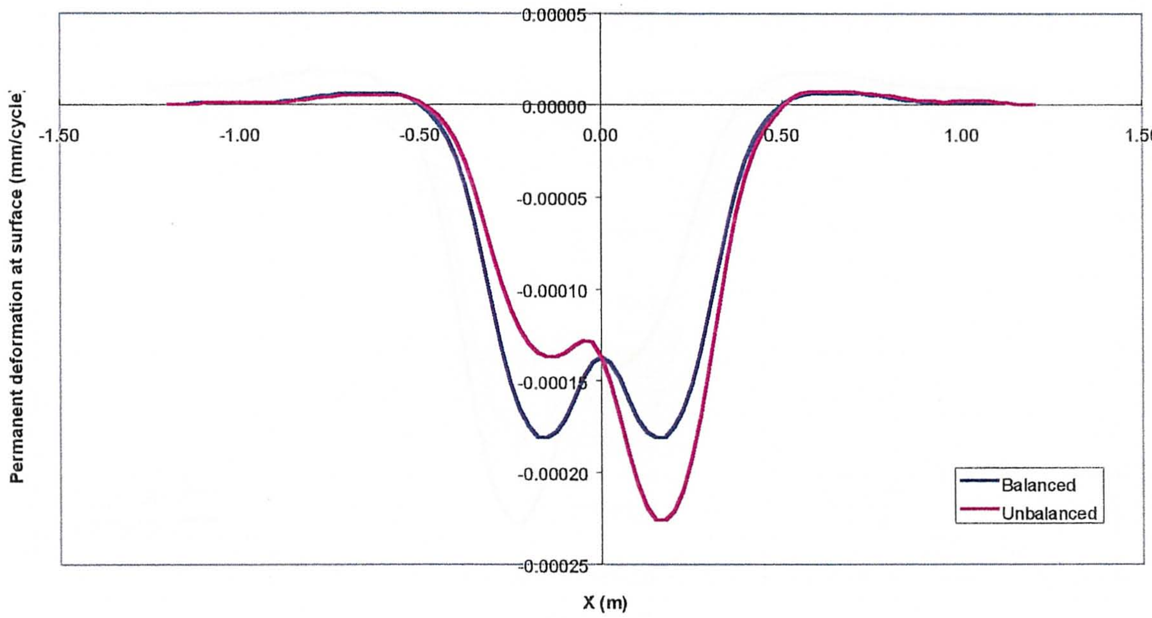

Figure A.34 – Permanent deformation by cycle at surface for the tyre 295/60R22.5 (9.0 ton / 8 bar) with balanced and unbalanced load in pavement 2 with the effect of the lateral wandering

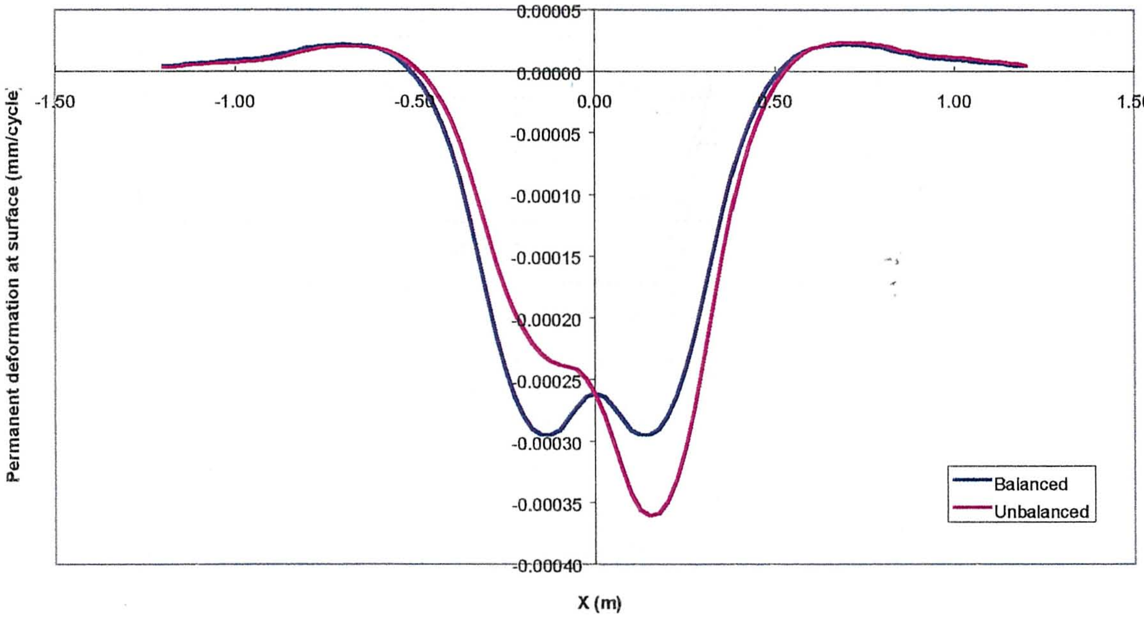

Figure A.35 – Permanent deformation by cycle at surface for the tyre 295/60R22.5 (9.0 ton / 8 bar) with balanced and unbalanced load in pavement 3 with the effect of the lateral wandering

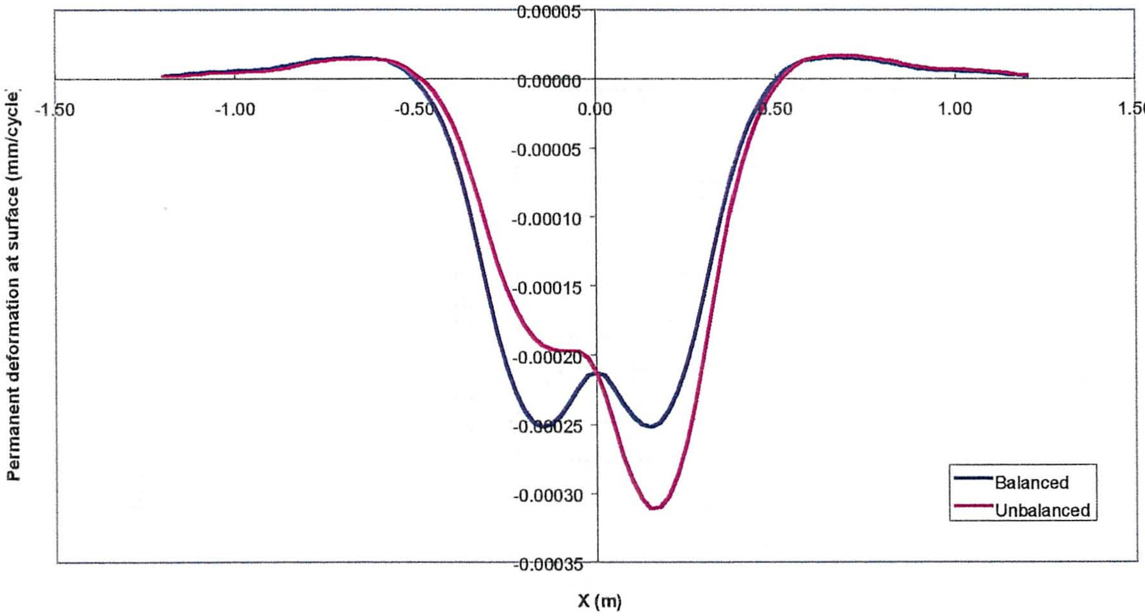

Figure A.36 – Permanent deformation by cycle at surface for the tyre 295/60R22.5 (9.0 ton / 8 bar) with balanced and unbalanced load in pavement 4 with the effect of the lateral wandering

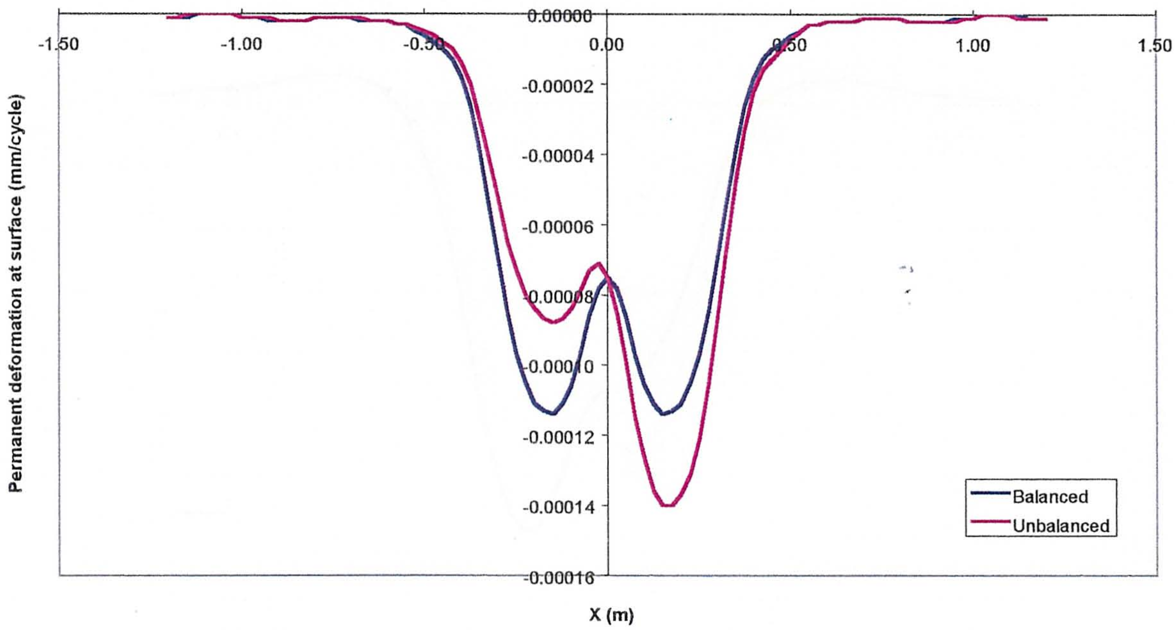

Figure A.37 – Permanent deformation by cycle at surface for the tyre 295/60R22.5 (11.5 ton / 10 bar) with balanced and unbalanced load in pavement 1 with the effect of the lateral wandering

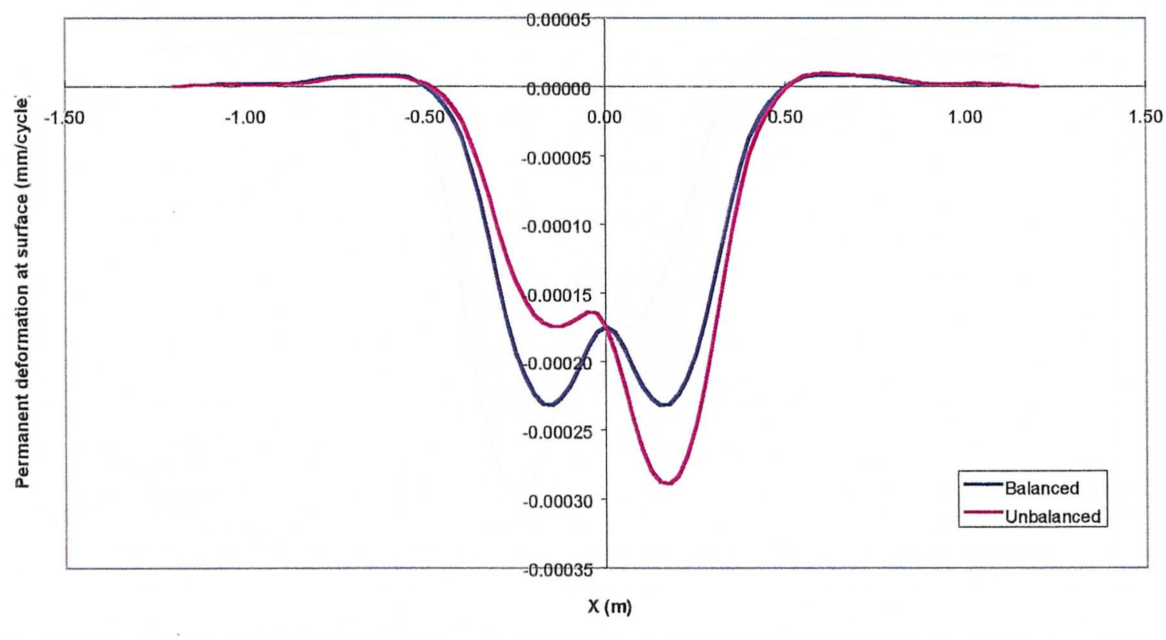

Figure A.38 – Permanent deformation by cycle at surface for the tyre 295/60R22.5 (11.5 ton / 10 bar) with balanced and unbalanced load in pavement 2 with the effect of the lateral wandering

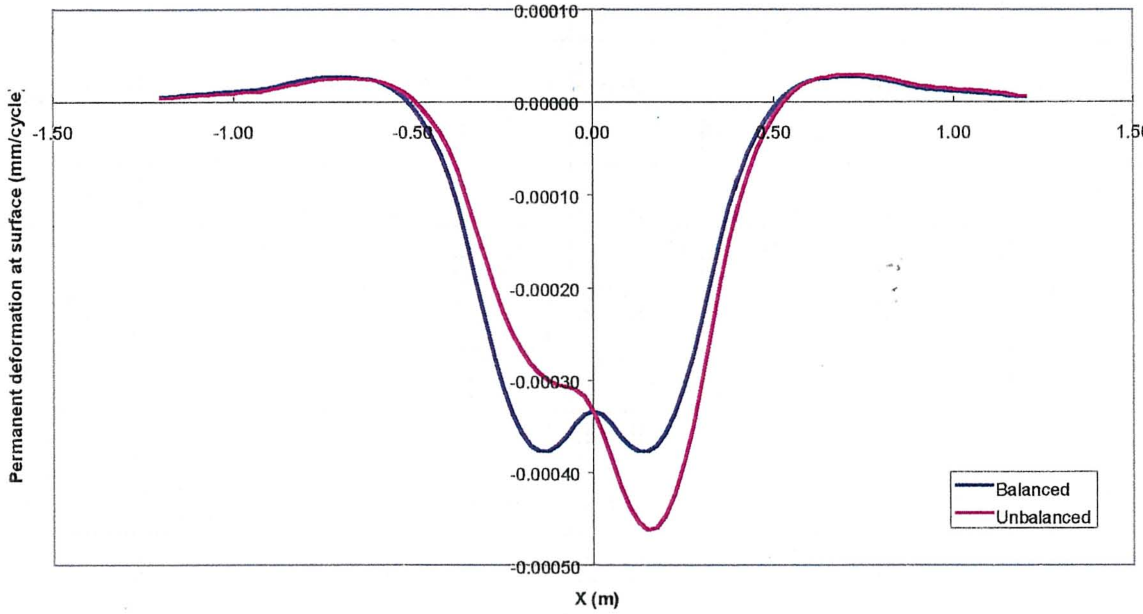

Figure A.39 – Permanent deformation by cycle at surface for the tyre 295/60R22.5 (11.5 ton / 10 bar) with balanced and unbalanced load in pavement 3 with the effect of the lateral wandering

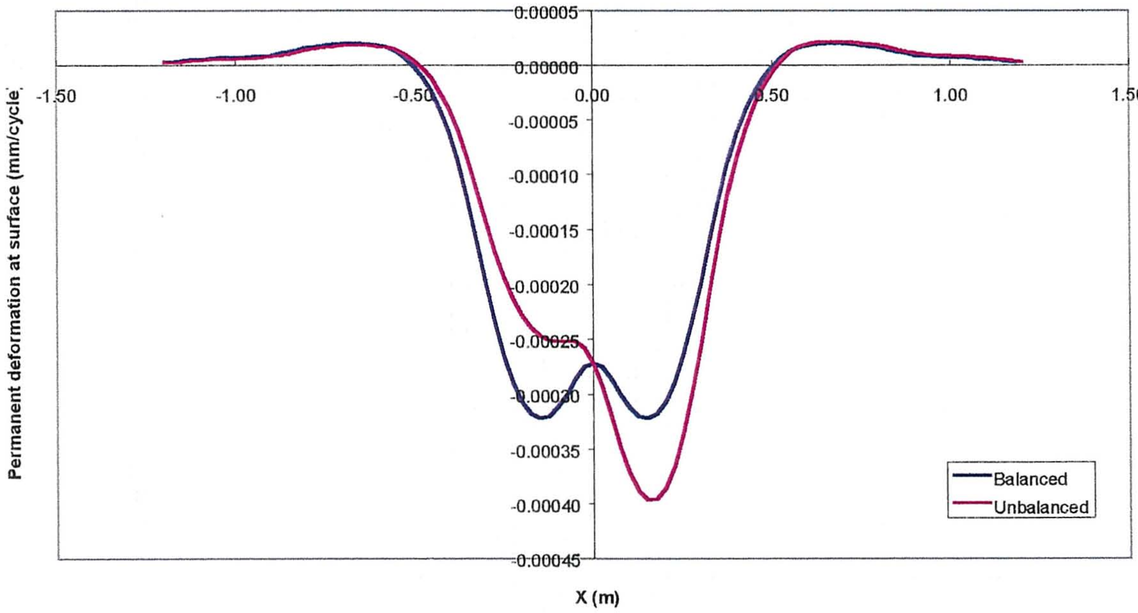

Figure A.40 – Permanent deformation by cycle at surface for the tyre 295/60R22.5 (11.5 ton / 10 bar) with balanced and unbalanced load in pavement 4 with the effect of the lateral wandering

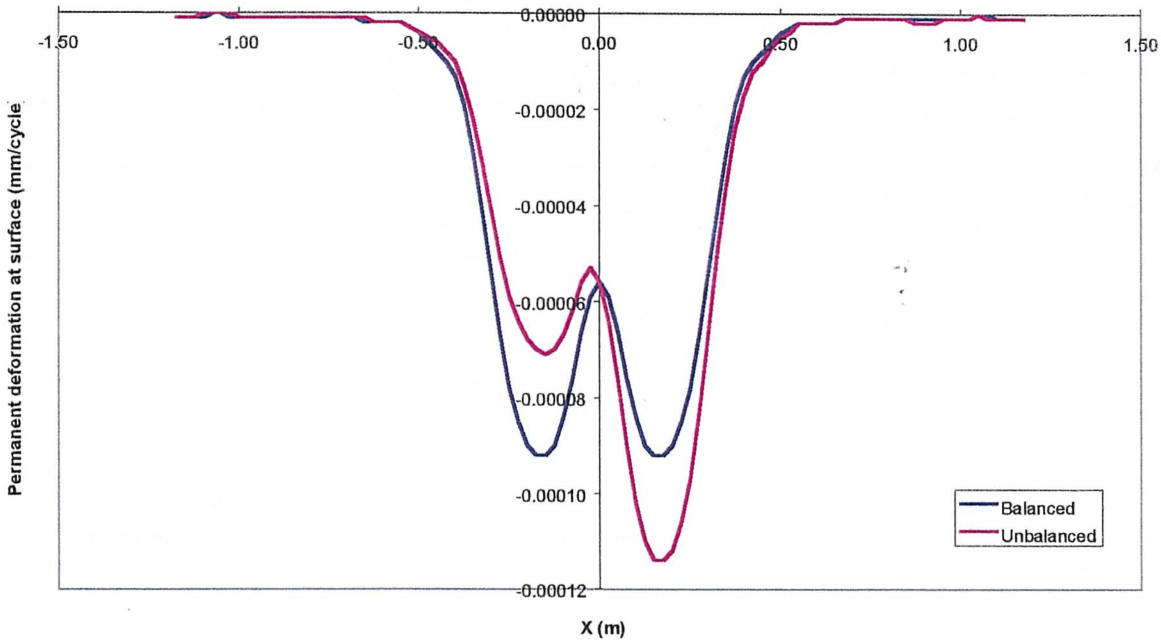

Figure A.41 – Permanent deformation by cycle at surface for the tyre 295/80R22.5 (9.0 ton / 7 bar) with balanced and unbalanced load in pavement 1 with the effect of the lateral wandering

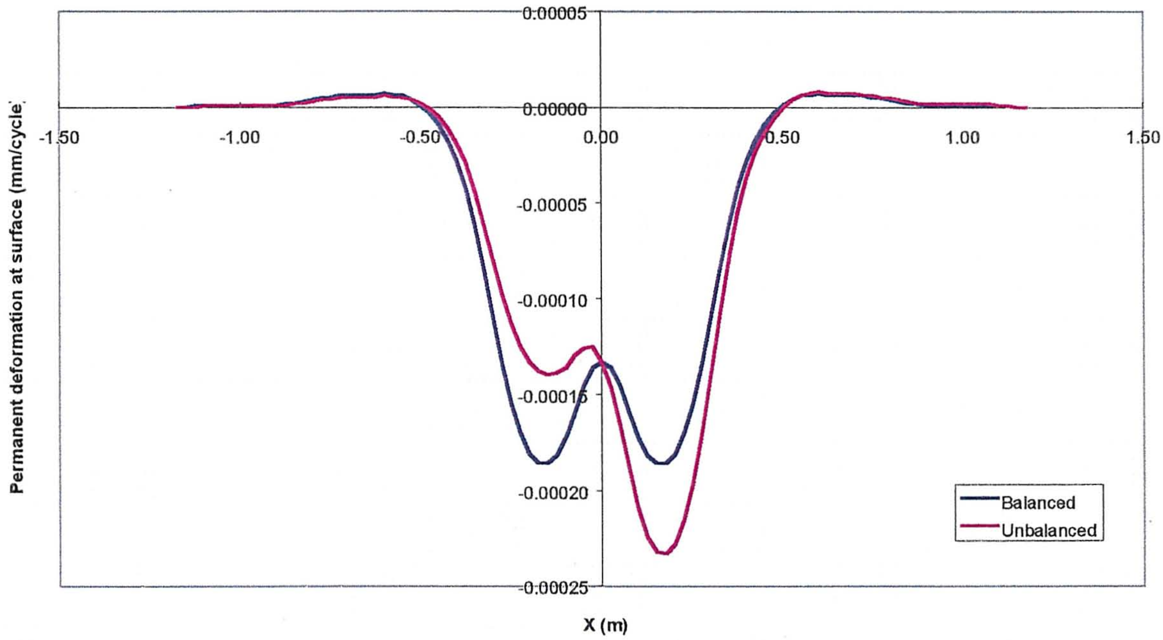

Figure A.42 – Permanent deformation by cycle at surface for the tyre 295/80R22.5 (9.0 ton / 7 bar) with balanced and unbalanced load in pavement 2 with the effect of the lateral wandering

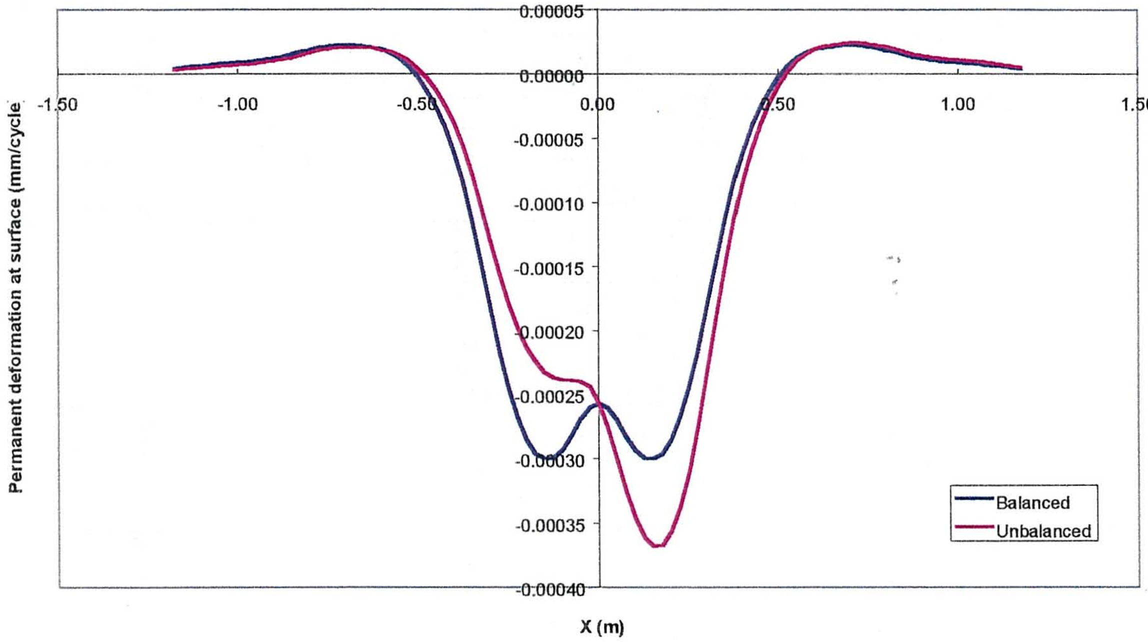

Figure A.43 – Permanent deformation by cycle at surface for the tyre 295/80R22.5 (9.0 ton / 7 bar) with balanced and unbalanced load in pavement 3 with the effect of the lateral wandering

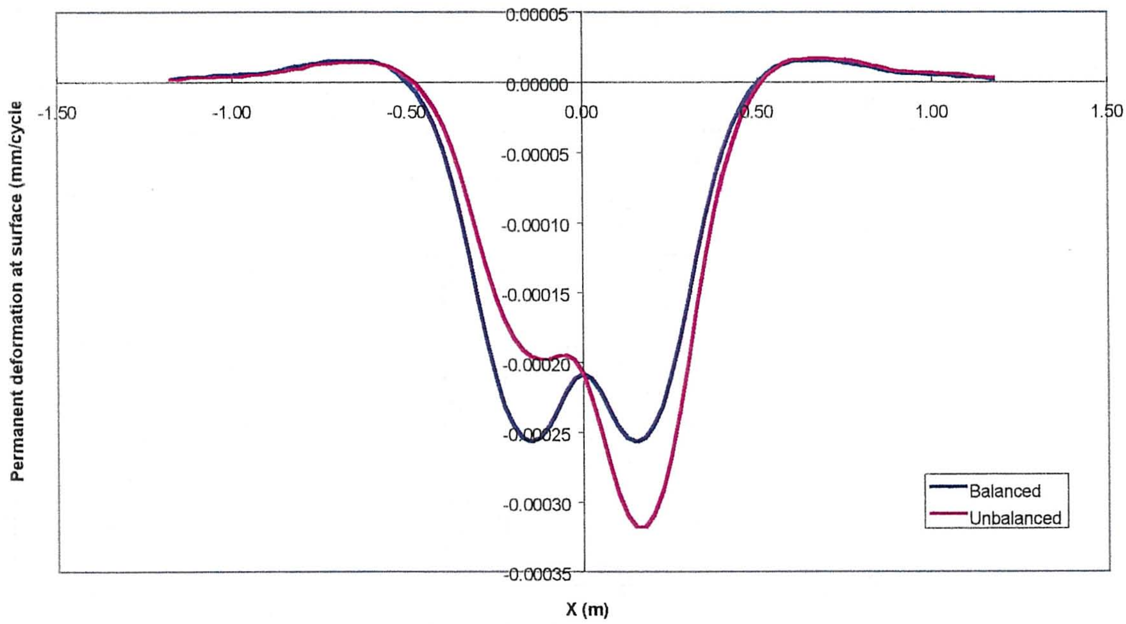

Figure A.44 – Permanent deformation by cycle at surface for the tyre 295/80R22.5 (9.0 ton / 7 bar) with balanced and unbalanced load in pavement 4 with the effect of the lateral wandering

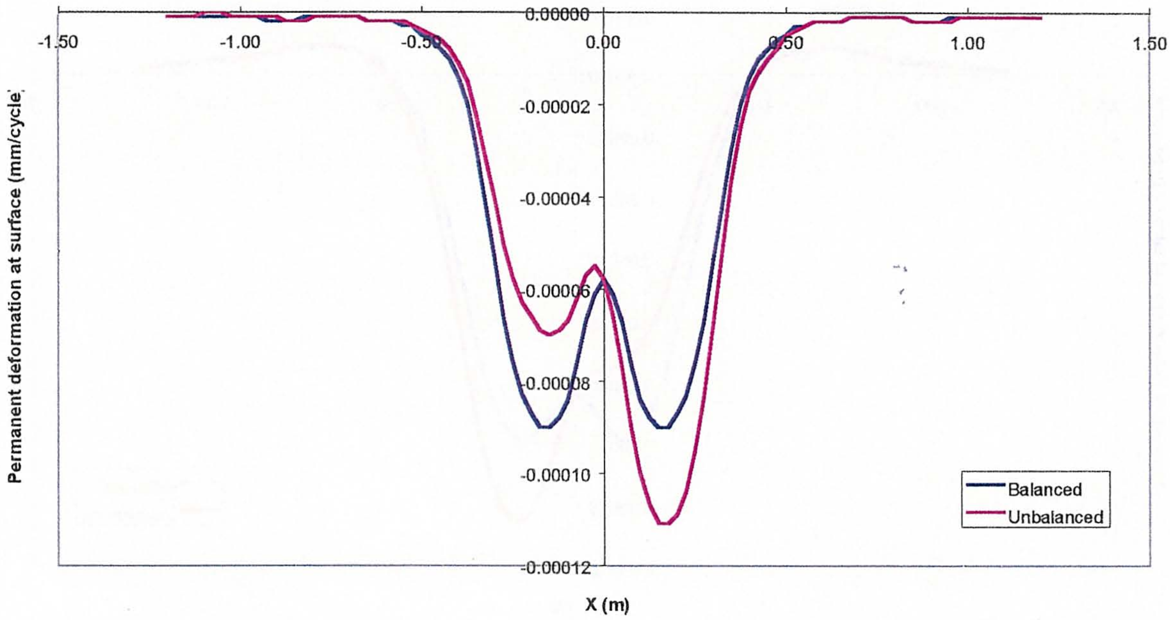

Figure A.45 – Permanent deformation by cycle at surface for the tyre 315/80R22.5 (9.0 ton / 6.5 bar) with balanced and unbalanced load in pavement 1 with the effect of the lateral wandering

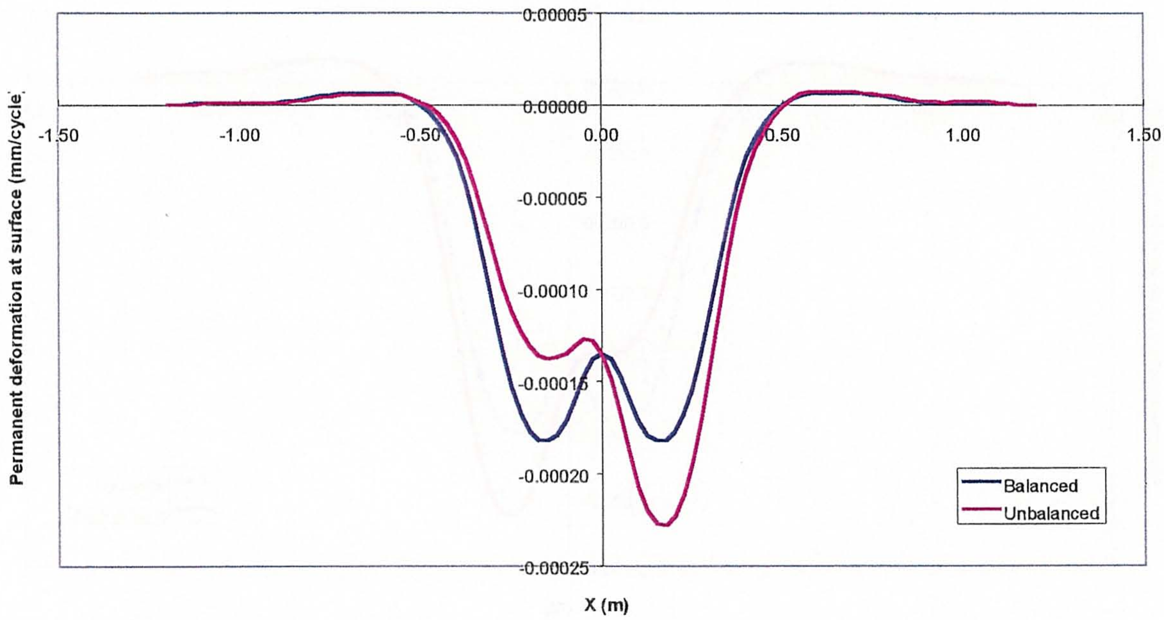

Figure A.46 – Permanent deformation by cycle at surface for the tyre 315/80R22.5 (9.0 ton / 6.5 bar) with balanced and unbalanced load in pavement 2 with the effect of the lateral wandering

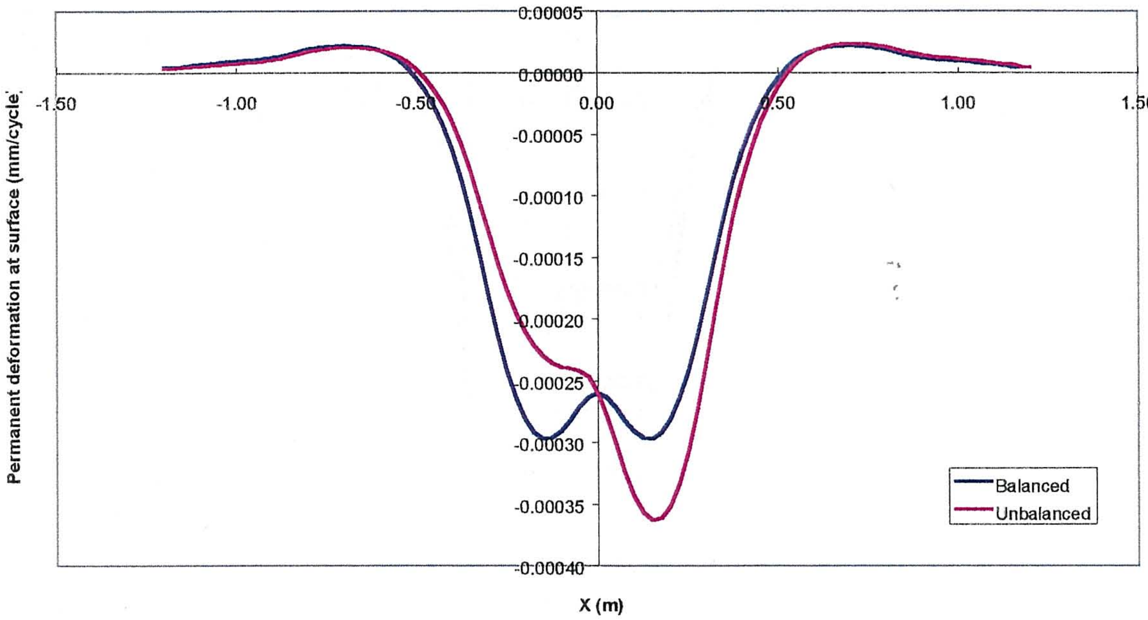

Figure A.47 – Permanent deformation by cycle at surface for the tyre 315/80R22.5 (9.0 ton / 6.5 bar) with balanced and unbalanced load in pavement 3 with the effect of the lateral wandering

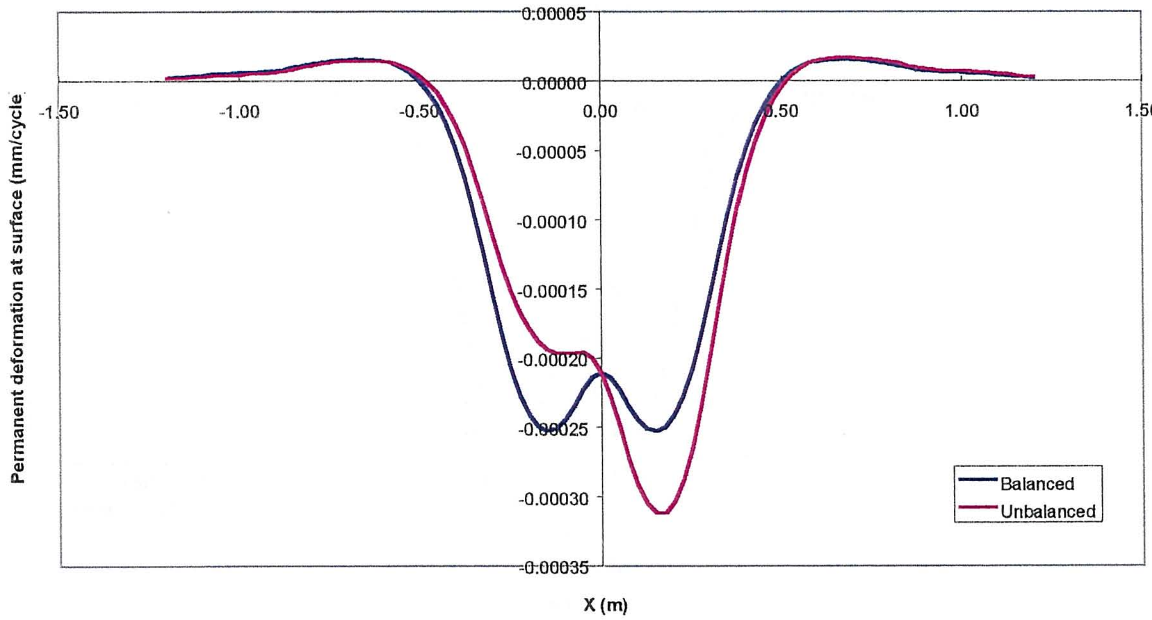

Figure A.48 – Permanent deformation by cycle at surface for the tyre 315/80R22.5 (9.0 ton / 6.5 bar) with balanced and unbalanced load in pavement 4 with the effect of the lateral wandering

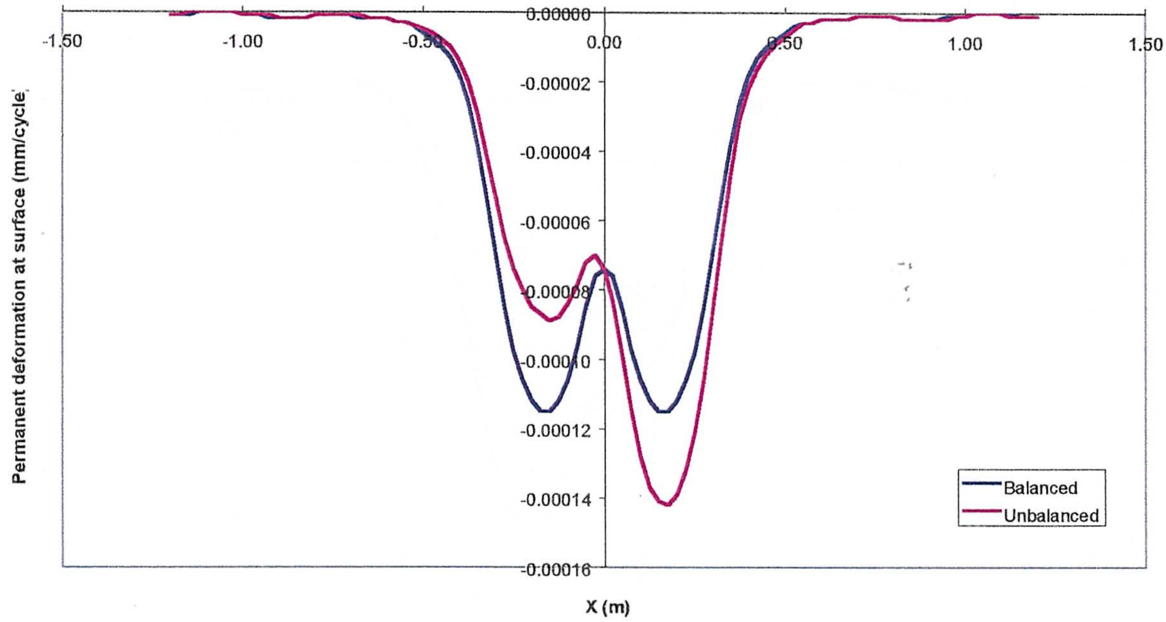

Figure A.49 – Permanent deformation by cycle at surface for the tyre 315/80R22.5 (11.5 ton / 8 bar) with balanced and unbalanced load in pavement 1 with the effect of the lateral wandering

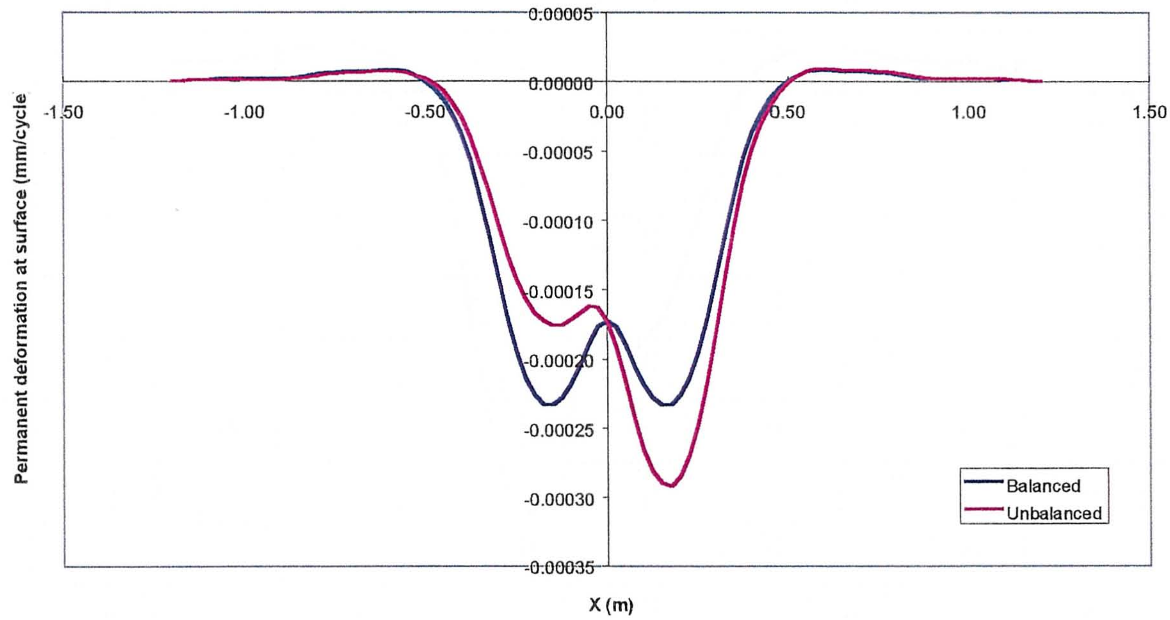

Figure A.50 – Permanent deformation by cycle at surface for the tyre 315/80R22.5 (11.5 ton / 8 bar) with balanced and unbalanced load in pavement 2 with the effect of the lateral wandering

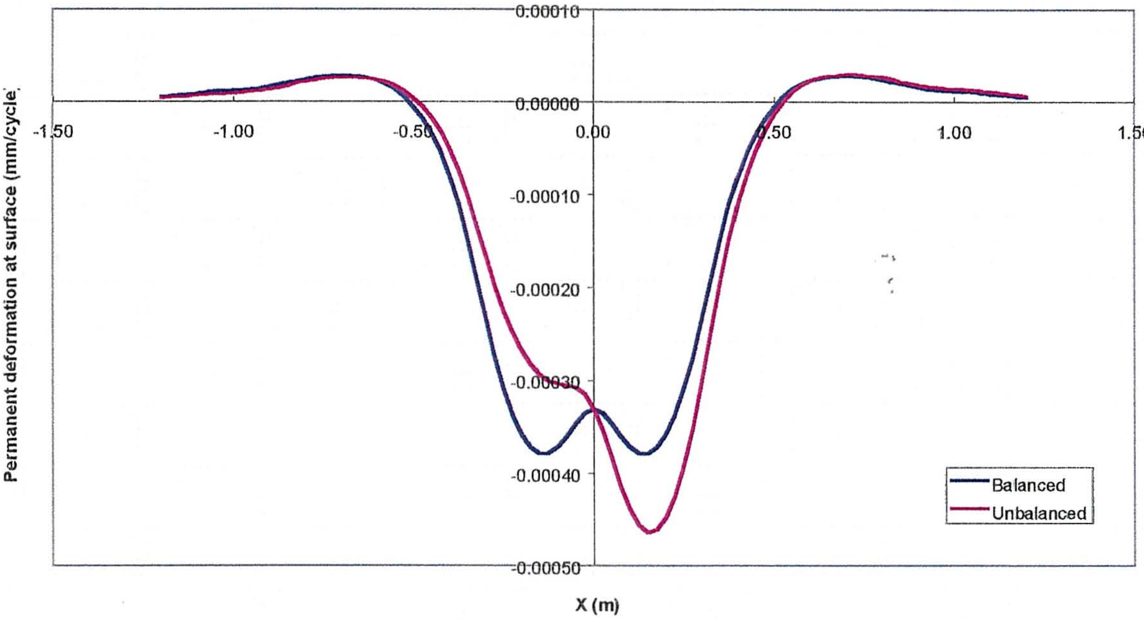

Figure A.51 – Permanent deformation by cycle at surface for the tyre 315/80R22.5 (11.5 ton / 8 bar) with balanced and unbalanced load in pavement 3 with the effect of the lateral wandering

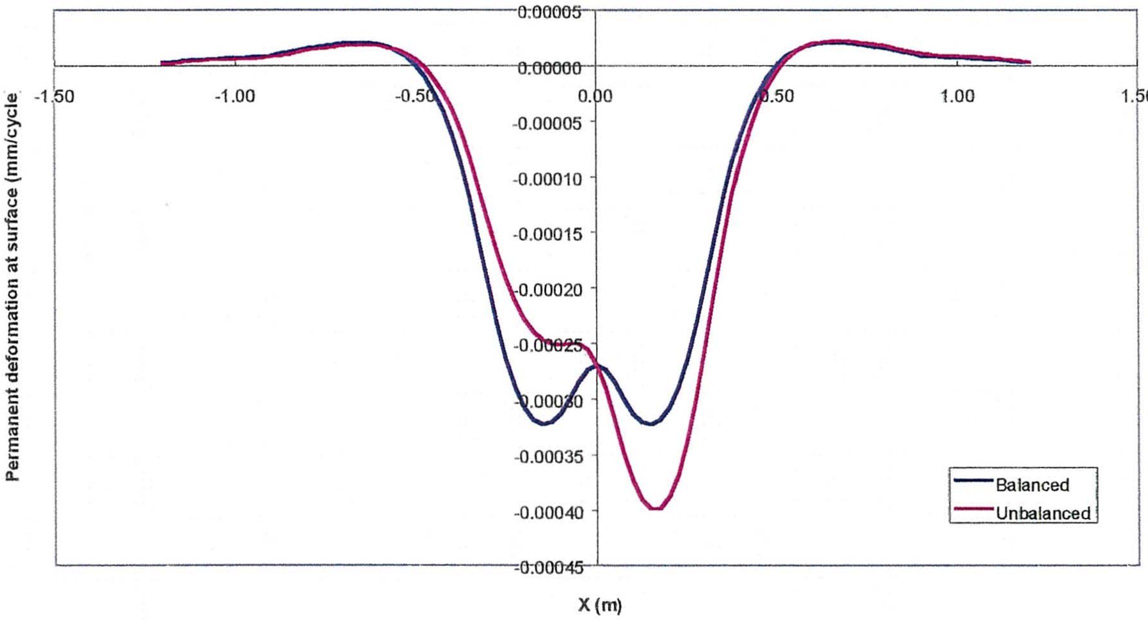

Figure A.52 – Permanent deformation by cycle at surface for the tyre 315/80R22.5 (11.5 ton / 8 bar) with balanced and unbalanced load in pavement 4 with the effect of the lateral wandering

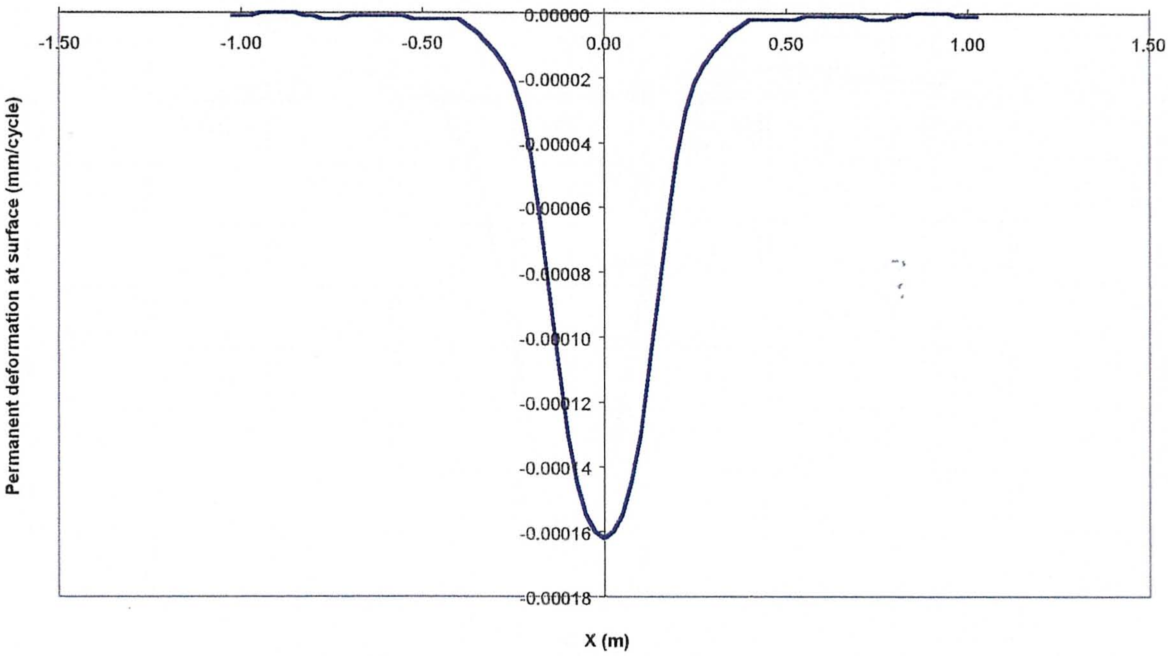

Figure A.53 – Permanent deformation by cycle at surface for the tyre 385/65R22.5 (9.0 ton / 10 bar) in pavement 1 with the effect of the lateral wandering

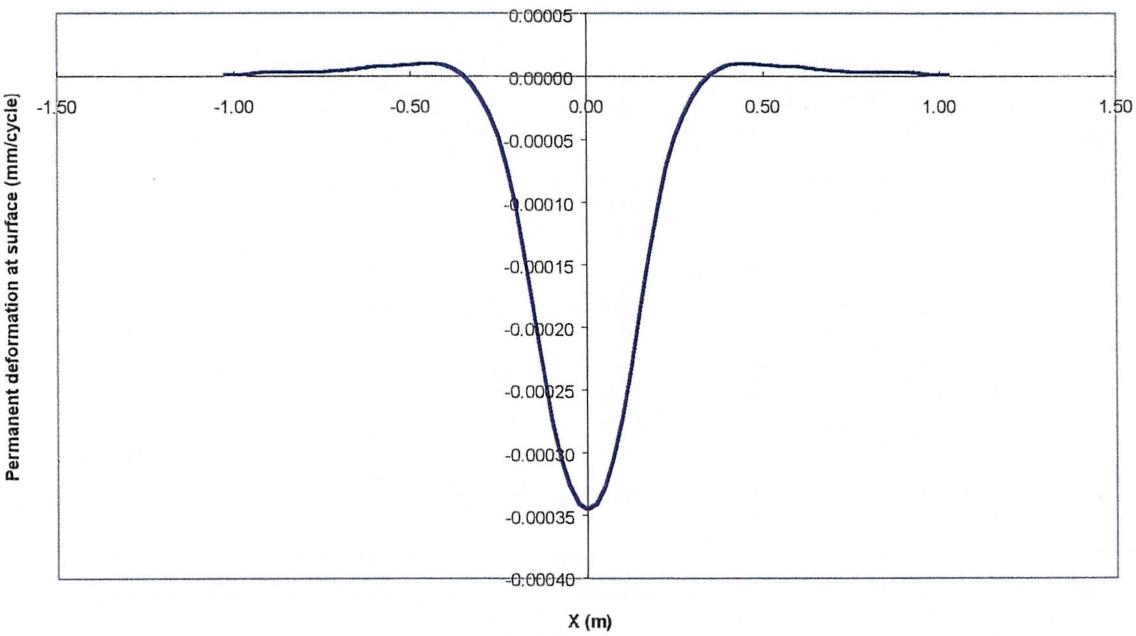

Figure A.54 – Permanent deformation by cycle at surface for the tyre 385/65R22.5 (9.0 ton / 10 bar) in pavement 2 with the effect of the lateral wandering

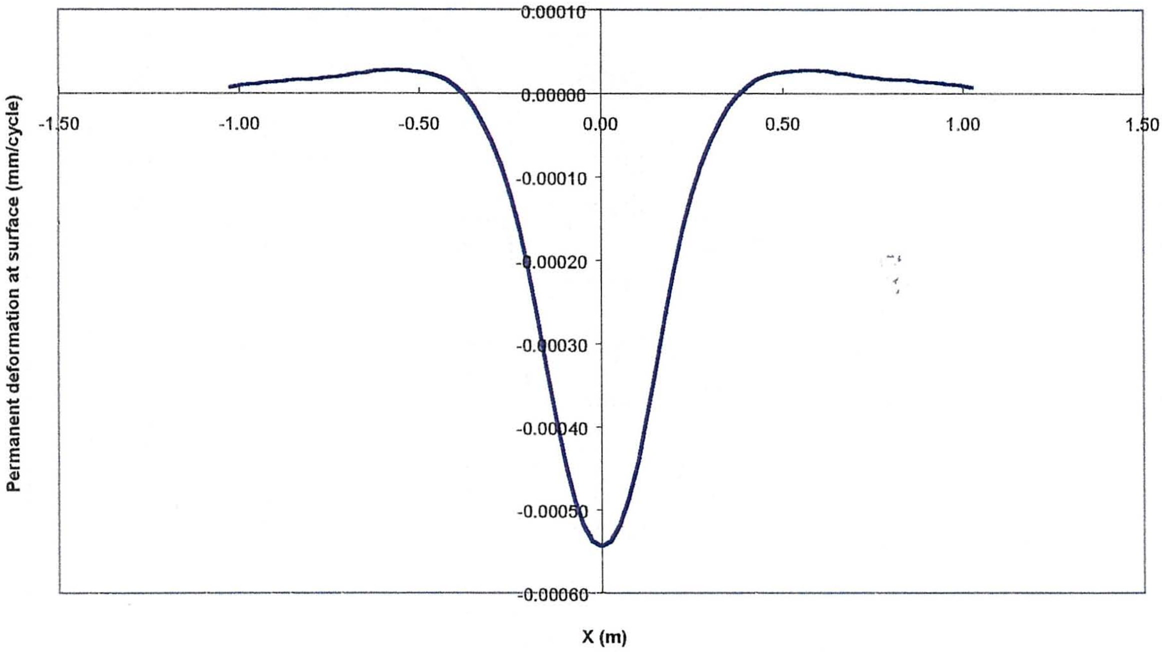

Figure A.55 – Permanent deformation by cycle at surface for the tyre 385/65R22.5 (9.0 ton / 10 bar) in pavement 3 with the effect of the lateral wandering

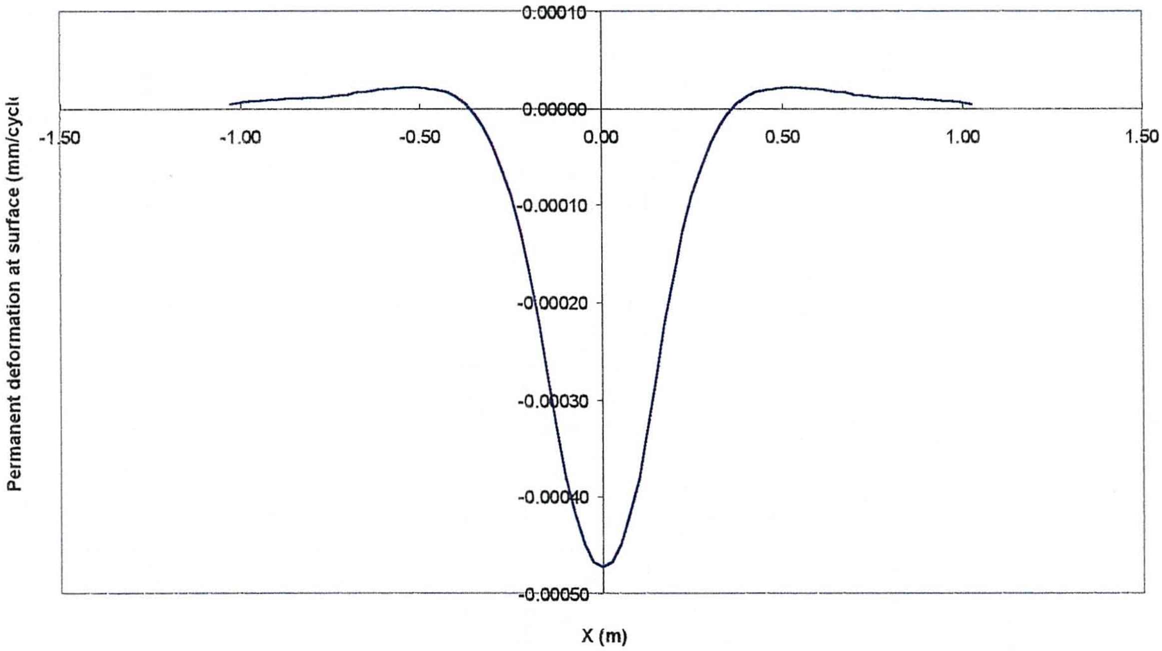

Figure A.56 – Permanent deformation by cycle at surface for the tyre 385/65R22.5 (9.0 ton / 10 bar) in pavement 4 with the effect of the lateral wandering

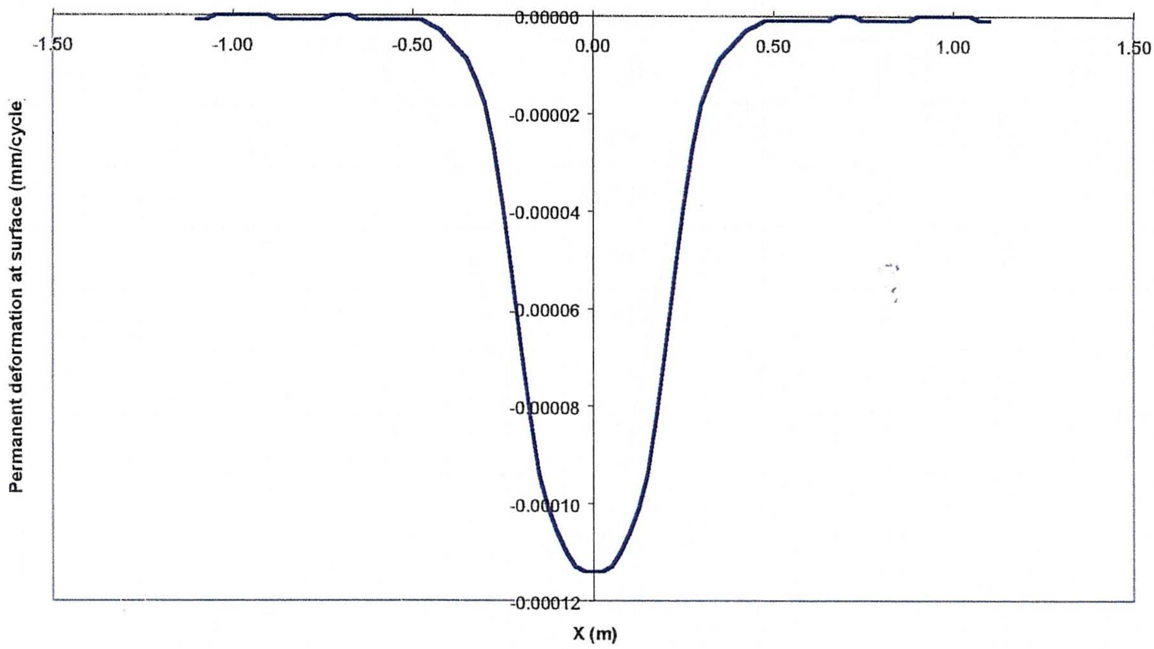

Figure A.57 – Permanent deformation by cycle at surface for the tyre 495/45R22.5 (9.0 ton / 8 bar) in pavement 1 with the effect of the lateral wandering

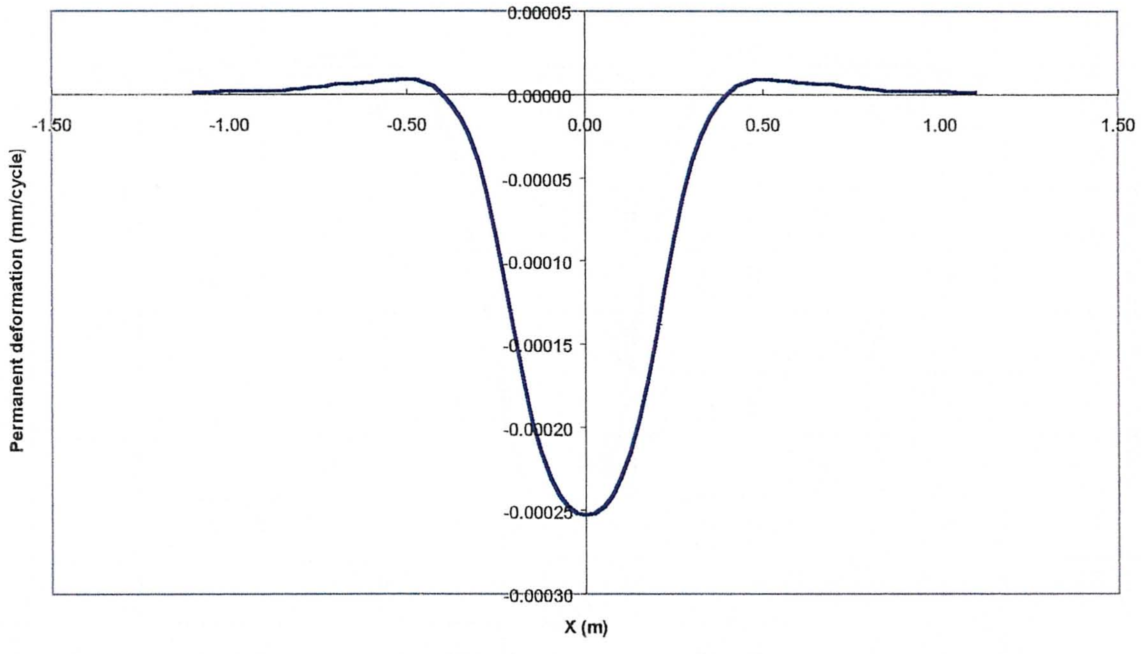

Figure A.58 – Permanent deformation by cycle at surface for the tyre 495/45R22.5 (9.0 ton / 8 bar) in pavement 2 with the effect of the lateral wandering

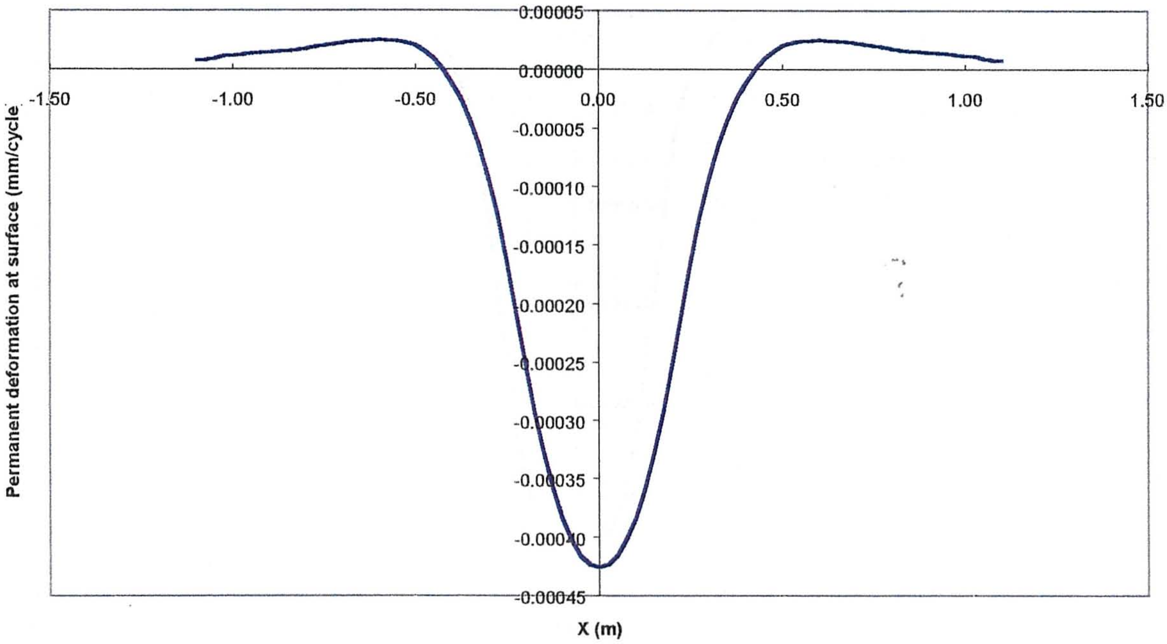

Figure A.59 – Permanent deformation by cycle at surface for the tyre 495/45R22.5 (9.0 ton / 8 bar) in pavement 3 with the effect of the lateral wandering

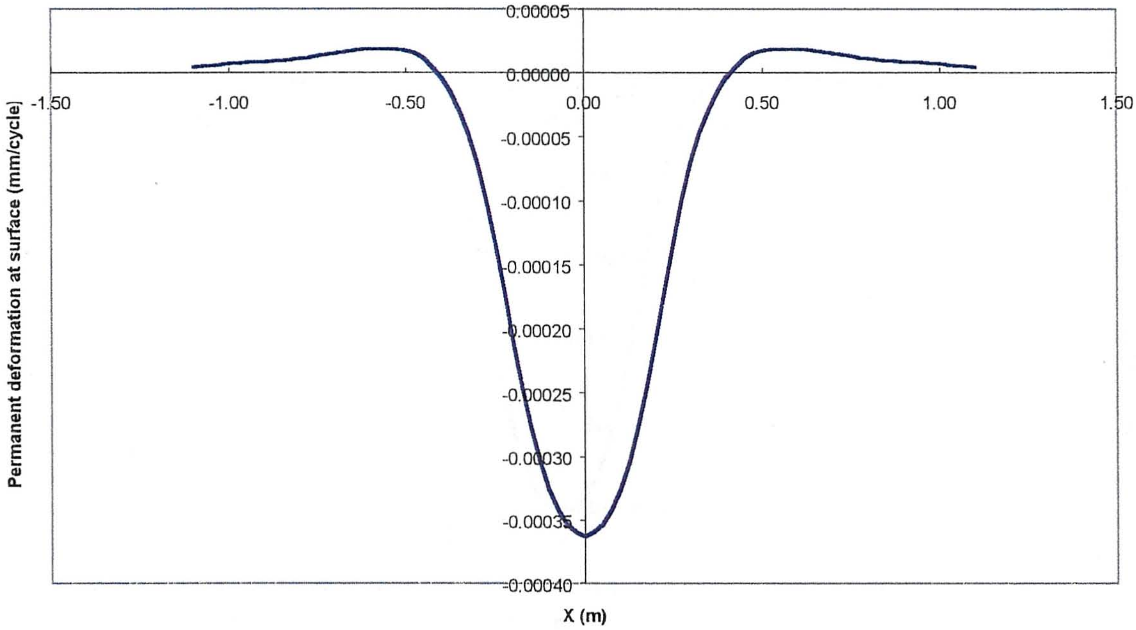

Figure A.60 – Permanent deformation by cycle at surface for the tyre 495/45R22.5 (9.0 ton / 8 bar) in pavement 4 with the effect of the lateral wandering

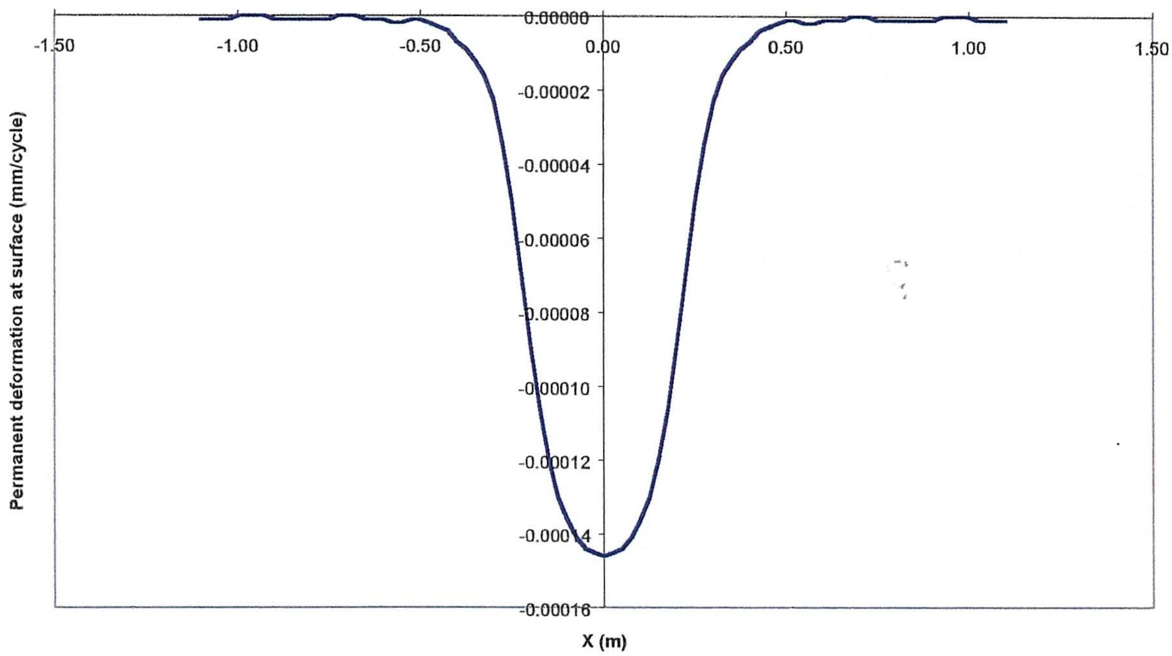

Figure A.61 – Permanent deformation by cycle at surface for the tyre 495/45R22.5 (11.5 ton / 10 bar) in pavement 1 with the effect of the lateral wandering

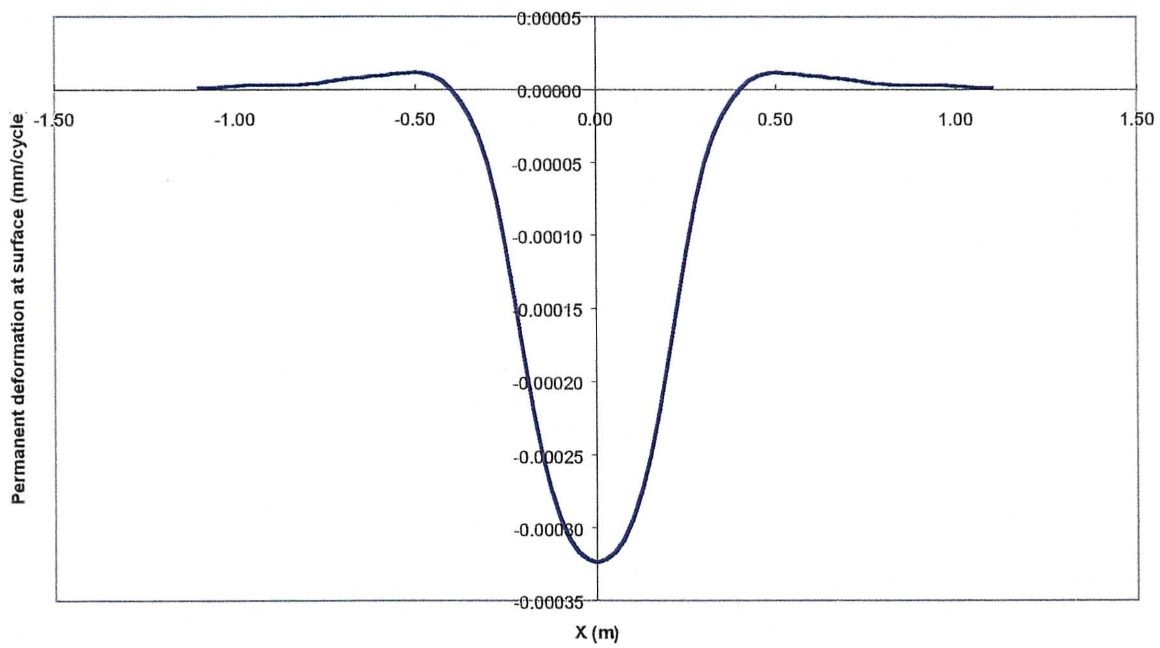

Figure A.62 – Permanent deformation by cycle at surface for the tyre 495/45R22.5 (11.5 ton / 10 bar) in pavement 2 with the effect of the lateral wandering

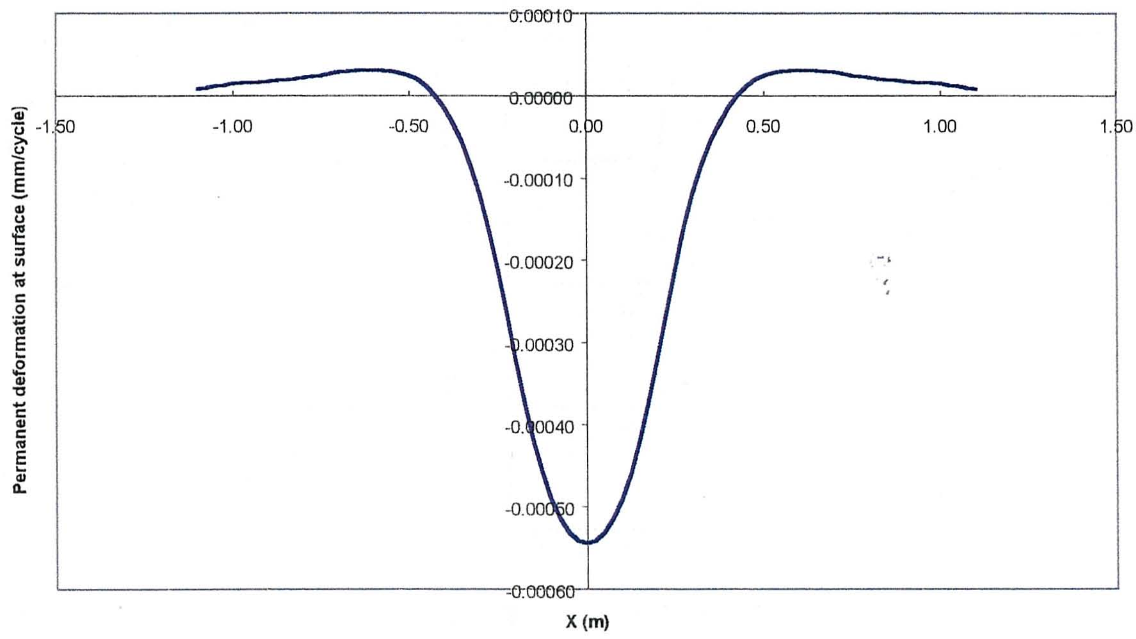

Figure A.63 – Permanent deformation by cycle at surface for the tyre 495/45R22.5 (11.5 ton / 10 bar) in pavement 3 with the effect of the lateral wandering

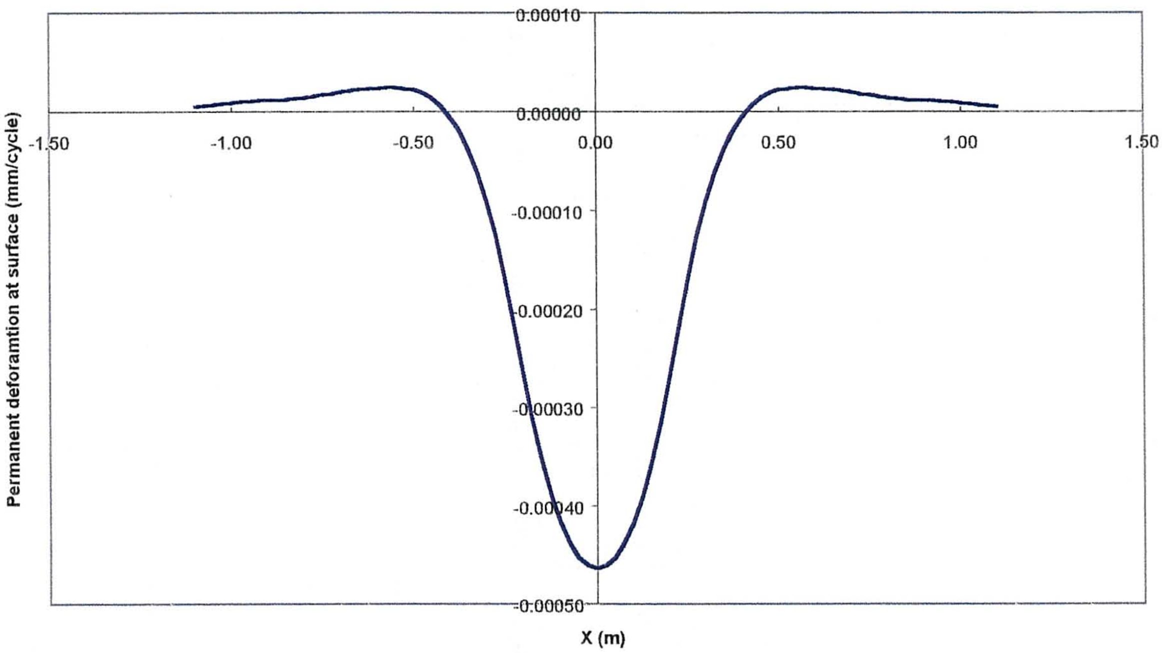

Figure A.64 – Permanent deformation by cycle at surface for the tyre 495/45R22.5 (11.5 ton / 10 bar) in pavement 4 with the effect of the lateral wandering

Sector de Edições e Artes Gráficas do LNEC